



UNIVERSITY OF ROME
"TOR VERGATA"

FACULTY OF SCIENCE

DOCTORATE DEGREE IN CHEMICAL SCIENCES
XXI CYCLE

NEW PHYSIOLOGICAL ROLES OF
GLUTATHIONE TRANSFERASES

Kutayba Farhan Dawood

2008/2009

Supervisor: Prof. Giorgio Ricci

Coordinator: Prof. Bruno Crociani

ACKNOWLEDGMENTS

First, all praise and thanks to God Almighty – ALLAH. I would like to thank the Italian Ministry of Foreign Affairs.

I would like to record my gratitude to Prof. Giorgio Ricci for his supervision, advice, and guidance from the very early stage of this research as well as giving me extraordinary experiences throughout the work. Above all and the most needed, he provided me unflinching encouragement and support in various ways.

Special thank to my friend Dr. Raffaele Fabrini for all his assistances, as a brother.

Lastly, and most importantly, I wish to thank my parents. They bore me, raised me, supported me, taught me, and loved me. To them I dedicate this thesis. To my wife, and our daughter, all I can say is it would take another thesis to express my deep love for you.

TABLE OF CONTENTS

| | |
|--|----|
| ABSTRACT | 5 |
| ABBREVIATIONS | 6 |
| 1. GLUTATHIONE TRANSFERASE | |
| <i>General Introduction</i> | 8 |
| 1.1 Glutathione Transferases (GSTs) | 9 |
| 1.2 Classification of Glutathione Transferases | 9 |
| 1.3 GST of the malarial parasites | 10 |
| 1.4 GST enzymatic functions | 11 |
| 1.5 Ligandin properties | 13 |
| 1.6 Apoptosis regulation | 14 |
| 1.7 GSTs structures | 14 |
| 1.7.1 Mammalian cytosolic GST | 14 |
| 1.7.2 GST of human malarial parasites (<i>Plasmodium falciparum</i>) | 17 |
| 1.8 GSTs and Nitric Oxide | 19 |
| 1.8.1 Nitric oxide (Nitrogen monoxide) | 19 |
| 1.8.2 Dinitrosyl iron complex | 20 |
| 1.9 References | 23 |
| AIM OF THESIS | 32 |
| 2. STUDY OF THE INTERACTION BETWEEN GSTs AND DNDGIC IN INTACT CELLS AND TISSUES | 33 |
| 2.1 Introduction | 34 |
| 2.2 Experimental Procedures | 36 |
| 2.3 Results | 40 |
| 2.4 Discussion | 50 |
| 2.5 References | 53 |

| | |
|--|-----------|
| 3. STUDY OF GST LOCALIZATION IN NUCLEI AND SUBCELLULAR FRACTIONS OF RAT | 55 |
| 3.1 Introduction | 56 |
| 3.2 Experimental Procedures | 57 |
| 3.3 Results | 61 |
| 3.4 Discussion | 72 |
| 3.5 References | 76 |
| 4. STUDY OF GST OF MALARIAL PARASITE (<i>Plasmodium falciparum</i>) | 79 |
| 4.1 Introduction | 80 |
| 4.2 Experimental Procedures | 82 |
| 4.3 Results | 85 |
| 4.4 Discussion | 95 |
| 4.5 References | 97 |
| CONCLUDING REMARKS | 98 |

ABSTRACT

Glutathione transferases (GSTs) are enzymes able to conjugate GSH to a lot of toxic compounds thereby favoring their excretion. Recently, other protective roles of these enzymes have been discovered. In particular, it has been observed that a peculiar and strong interaction exists between some mammalian GSTs and an endogenous carrier of nitric oxide, the dinitrosyl-diglutathionyl iron complex (DNDGIC). This iron complex is a paramagnetic molecule with a characteristic EPR spectrum centered at $g = 2.03$, that is spontaneously formed when NO enters the cell. This complex is a strong irreversible inhibitor of glutathione reductase. The present work explores the possible role of GSTs like a protection system against DNDGIC. Actually, mammalian GSTs bind DNDGIC with extraordinary affinity ($K_D = 10^{-9}$ - 10^{-10} M). When rat hepatocytes are incubated in the presence of GSNO, a natural source of NO, a rapid formation of 0.1 - 0.2 mM intracellular DNDGIC has been observed. This concentration would be lethal for glutathione reductase. However the complex does not appear like a free species but completely bound to GSTs, that are present at the cytosolic level of 0.8 mM. In this form the complex is completely harmless for glutathione reductase.

Surprisingly, electron paramagnetic data, reveal that DNGIC-GST is partially associated to subcellular fractions and in particular to nuclei. Our data indicate that about 10% of the cytosolic pool GST is electrostatically associated with the outer nuclear membrane, and a similar quantity is compartmentalized inside the nucleus. Mainly Alpha class GSTs, in particular GSTA1-1, GSTA2-2 and GSTA3-3, are involved in this double modality of interaction. Confocal microscopy and immunofluorescence experiments have been used to detail the electrostatic association in hepatocytes. A quantitative analysis of the membrane-bound Alpha GSTs suggests the existence of a multilayer

assembly of these enzymes at the outer nuclear envelope that could represent a potent protection shell for the nucleus and an amazing novelty in cell physiology.

A second target of this study is represented by the particular GST isoenzyme expressed by the *Plasmodium falciparum* (*PfGST*), the parasite causative of malaria. This enzyme is characterized by a peculiar dimer/tetramer transition that occurs in the absence of GSH and that causes a total loss of its enzymatic activity. Moreover *PfGST* binds hemin with high affinity and this interaction is finalized to the protection of the parasite against this toxic compound. Binding of hemin is regulated by a cooperative mechanism and does not occur in the tetrameric enzyme. Side directed mutagenesis, steady-state kinetic experiments, fluorescence anisotropy and X-ray crystallography were used to verify the involvement of some protein segment in the tetramerization process and in the cooperative phenomenon. Actually the loop 113-118 represents one the most prominent structural difference between *PfGST* and other GSTs. Our results demonstrate that truncation, increased rigidity or even a simple point mutation of this loop cause a dramatic change of the tetramerization kinetics that becomes hundred times slower than that observed in the native enzyme. Furthermore all mutants loose the positive cooperativity for hemin binding found in the native structure suggesting that the integrity of this peculiar loop is essential for intersubunit communication. Interestingly, the tetramerization process, that is very fast in the absence of GSH in the native enzyme, is prevented not only by GSH but even by GSSG. This result indicate that the protection of the parasite against free hemin is independent of the redox status of the cell.

ABBREVIATIONS

| | |
|---------------|---|
| CDNB | 1-Chloro-2,4-dinitrobenzene |
| CEM | Human acute lymphoblastic T-cell leukemia Cell |
| DNDGIC | Dinitrosyl-diglutathionyl iron complex |
| EPR | Electron Paramagnetic Resonance |
| GSH | Glutathione (γ -glutamyl-cysteinyl-glycine) |
| GSNO | S-Nitrosoglutathione |
| GSSG | Glutathione Reductase |
| GST | Glutathione Transferase |
| JNK | Jun N-terminal kinase |
| MAPEG | Membrane Associated Proteins in Eicosanoid and Glutathione metabolism |
| NBD-Cl | 4-chloro-7-nitro-2,1,3-benzoxadiazole |
| NBDHEX | 6-(7-Nitro-2,1,3-benzoxadiazol-4-ylthio)hexanol |
| NOS | Nitric Oxide Synthase |
| <i>Pf</i> GST | GST of <i>Plasmodium falciparum</i> parasite |
| SDS-PAGE | Sodium Dodecyl Sulphate - Poly Acrylamide Gel Electrophoresis |

1. GLUTATHIONE TRANSFERASE

General Introduction

1.1 Glutathione Transferases (GSTs)

Glutathione transferases are a superfamily of multifunctional enzymes that catalyze the addition of the nucleophilic thiol GSH (the tripeptide γ -glutamyl-cysteinyl-glycine) to xenobiotic and endogenous compounds which have electrophilic centers. Their substrates include alkyl and aryl halides, carboxylates, sulphate and phosphate esters, epoxides, organic nitrates, lactones, quinones, ozonides, thiocyanates and hydroperoxides (1-5). GSTs are involved in phase II of the mechanism of cellular detoxification. These proteins are found in all eukaryotic and prokaryotic systems, in the cytoplasm, in the microsomes and in mitochondria (6, 7). In human cells GSTs are present in high concentrations. For example in hepatocytes they represent about 3 - 5% of all cytosolic proteins. The GSTs are ubiquitous, especially abundant in the liver, lungs, in the placenta and skin (8, 9).

1.2 Classification of Glutathione Transferases

Over 100 different isoenzymes of GST have been described in species ranging from microorganisms to humans. Currently cytosolic GSTs are grouped into 12 isoenzymatic classes based on amino acid sequences, immunological properties and substrate and inhibitor specificity (10, 11).

A particular class is represented by the microsomal GST (MAPEG). This isoenzyme is associated to the microsomal membrane, and displays a peculiar trimeric structure (12). The cytosolic and mitochondrial GSTs are involved in the metabolism of xenobiotics, as well as in the detoxification against endogenous toxic compounds. In contrast, MAPEG is not involved in detoxification processes, but is active in the synthesis of prostaglandins and leukotrienes (5, 12).

In mammals 8 families of cytosolic GSTs are expressed, termed Alpha, Mu, Omega, Pi, Sigma, Theta and Zeta. Several other soluble GST classes have been reported: Delta and Epsilon in insects (13); Phi, Tau, Lambda in plants (14); Beta (15) and Chi in bacteria (16). The first classes discovered in mammals, *i.e.* Alpha, Mu and Pi, (17), are also the most advanced from an evolutionary point of view. The Alpha and Mu GST class are particularly abundant in the liver. The Alpha class GST plays also an additional detoxification role showing a peroxidase activity with organic peroxides. The GSTA1-1 and GSTA2-2 isoforms are highly

substrate-promiscuous with catalytic activity toward many structurally unrelated toxins (18-22) and the GSTA3-3 is involved in steroid biosynthesis and the metabolism of some xenobiotics (23).

1.3 GST of the malarial parasites

GST isoenzymes play a crucial role in parasites as they represent the main detoxification system due to the lack of Cytochrome P450 activity. A curious exception is represented by some protozoans such as *Trypanosoma cruzi*, *Trypanosoma brucei*, *Plasmodium berghei* and *Leishmania donovani* that replace the redox couple GSH/GSH reductase with trypanothione/trypanothione reductase (24-26). Furthermore, knockout studies in *Plasmodium falciparum* support the importance of functional cytosolic GSTs in these organisms (27). These findings place the parasite GSTs as targets for the development of new antiparasitic drugs (28, 29).

Tropical malaria, which is caused by the protozoan parasite *Plasmodium falciparum*, is responsible for about 515 million clinical cases (30) and one to three million deaths annually (31). The emergence and spread of drug resistance to commonly used chemotherapeutics are major factors contributing to this increasing burden. Thus, the characterization of alternative drug targets is urgently required (32-34). GST activity has been reported in all *Plasmodium* species studied so far as well as in all intraerythrocytic stages of the parasite (27).

The malaria parasite gives rise to disease only during its blood stage. This part of the lifecycle occurs largely within the red blood cell of the human host (35), where it digests a major proportion of the red cell hemoglobin (36). It has been demonstrated that *Plasmodium falciparum*, the causative agent of almost all fatal cases of malaria, detoxifies host hemoglobin-derived ferriprotoporphyrin IX in an acidic digestive vacuole mainly by converting it to hemozoin (37). Hemozoin is now known to be a crystalline cyclic dimer of ferriprotoporphyrin IX in which the propionate group of one porphyrin moiety coordinates to the Fe(III) center of its partner and vice-versa, while the second propionic acid group of each ferriprotoporphyrin IX hydrogen bonds to a neighboring dimer in the crystal (38).

Glutathione transferase of *Plasmodium falciparum* (*PfGST*) is the sole GST isoenzyme expressed by the parasite and it represents >1% of the total cellular protein (39, 40). A role of GST from *Plasmodium falciparum* in the development of drug resistance in malarial parasites has been postulated but is still controversial (28, 39). The *PfGST* differs significantly from human GSTs, and *PfGST* cannot be assigned to any of the previously known GST classes, thus representing a novel GST isoform (27, 29, 41-50) that may exert a particular protective role in the parasite. In fact, beside the usual activity that promote the conjugation of GSH to electrophilic toxic compounds, this protein binds efficiently hemin and thus it could protect the parasite (that lives in the erythrocytes) from the oxidative stress caused by residual free hemin that did not polymerize into hemozoin.

1.4 GST Enzymatic functions

GSTs display multifunctional nature because they are involved in different types of processes and have different enzyme activities (51). The main function is the transferase activity *i.e.* the reaction of conjugation of GSH to a wide variety of hydrophobic compounds, endobiotics or xenobiotics (Fig. 1.1), that have an electrophilic centre (4, 52, 53).

These electrophilic substrates include epoxides, alkyl and aryl halides, esters, activated alkenes, quinones and α , β -unsaturated carbonyls compounds (3, 41). With this conjugation the glutathione transferase plays the function of detoxification against of toxic compounds, both of endogenous nature, such as secondary metabolites of oxidative stress, both of exogenous nature, such as drugs, carcinogens, environmental pollutants, pesticides and herbicides. In addition to this specific activity, some isoforms also show a glutathione peroxidase selenium-independent activity, allowing them to catalyze the reduction of lipid hydroperoxide in the corresponding alcohols (54).

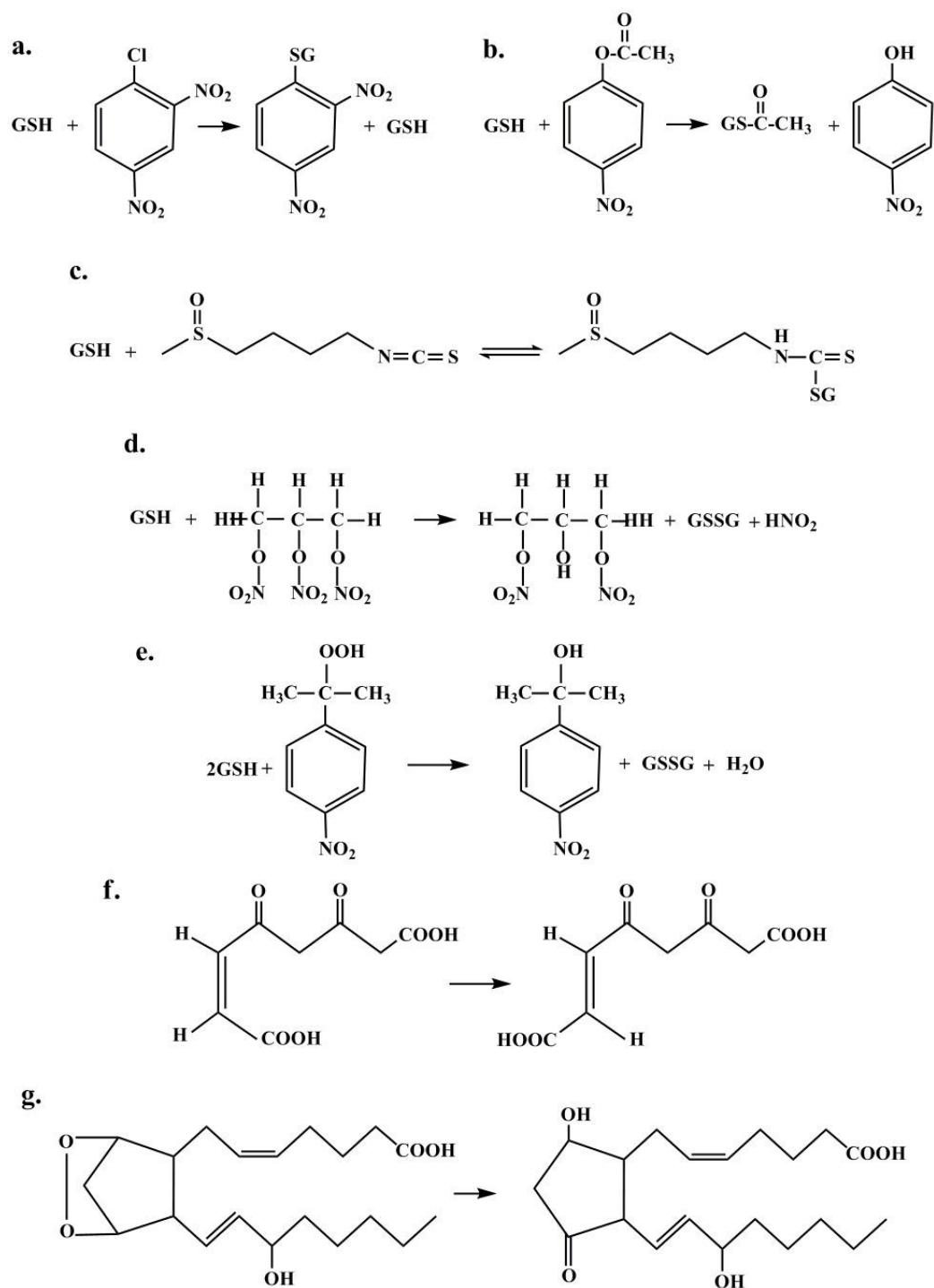


FIGURE 1.1. Reactions catalyzed by GSTs. Examples of conjugation, reduction, thiolysis, and isomerization reactions catalyzed by GST. The following substrates are shown: (a) chlorodinitrobenzene, (b) 4-nitrophenyl acetate, (c) sulforaphane (d) trinitroglycerin, (e) cumene hydroperoxide, (f) maleylacetoacetate, (g) prostaglandin PGH₂.

Thanks to this activity of peroxidation, combined with that of conjugation, the GSTs play an important role in the tissue protection process against oxidative damage (5). Other isoenzymes show an additional isomerase activity to various compounds such as unsaturated Δ^5 -3-chetosteroid, maleylacetoacetic acid and maleylacetone (Fig. 1.1). GSTs are also able to bind endogenous compounds such as leukotrienes and prostaglandins acting both in their catabolism, through the classic reaction of conjugation with the GSH (Fig. 1.2), and in their process of biosynthesis (55).

As an example of enzymatic mechanism is reported below the conjugation of GSH to the universal co-substrate 1-chloro-2,4-dinitrobenzene (CDNB):

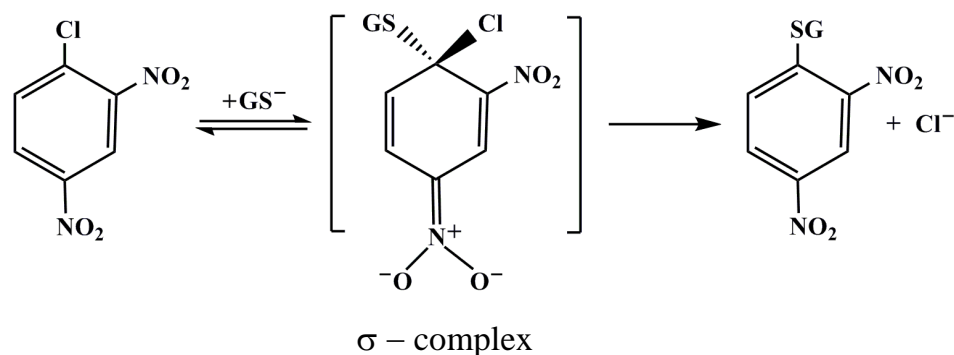


FIGURE 1.2. The conjugation of GSH to CDNB catalyzed by GSTs.

The catalysis of nucleophilic aromatic substitution reactions can be divided into steps involving binding of substrates to the enzyme active site, activation of GSH by deprotonation of the thiol to form the nucleophilic thiolate (56), and nucleophilic attack by the thiolate at the electrophilic center to form a σ -complex.

1.5 Ligandin properties

The panel of GSTs present in nature encompasses enzymes that catalyze conjugation, reduction and isomerase reactions, as well as proteins that act non-enzymatically as ligandines. Glutathione transferases are able to bind some hydrophobic compounds like bilirubin, heme, steroid and thyroid hormones. Some of these ligands neither bind to the G site nor to the H site, but to the interface of the two subunits, and the binding often inhibits glutathione transferases. This

interaction and compartmentalization prevents a possible cytotoxic accumulation in tissues of these lipophilic molecules (17).

1.6 Apoptosis regulation

Recently an important protein-protein interaction has been described involving GST and Jun N-terminal kinase (JNK), a protein involved in the cellular apoptotic process. Apoptosis is programmed cellular death primed from free JNK and other enzymes in cascade reactions. As long as JNK protein remains bound to the GST it is not in position to trigger cellular death. This GST-JNK interaction is regulated by their cytosolic concentrations. When the cell is in the increasing phase JNK is bound to GSTs and is inactive. Interaction with inhibitors, UV irradiation and oxidative stress, induce GSTs modification making the GST-JNK complex unstable. Therefore JNK becomes active priming the apoptotic process (57).

1.7 GSTs structures

1.7.1 Mammalian cytosolic GSTs

Representative tridimensional structures of at least one member from each cytosolic GSTs have been solved by X-ray diffraction studies (Fig. 1.3). The crystals were obtained in complex with the GSH (or its analogues) or inhibitors. All soluble GSTs display similar dimeric structures assembled mainly in α -helix (48-59%) and in minor measure by β -sheets (8-10%), the rest is constituted by regions irregularly structured and loops. Each subunit is constituted by two domains linked together by one peptide of a few amino acids. The first domain in these enzymes is located in the N-terminal portion and is responsible for GSH binding, hence the name "G-site". The domain is conserved for all classes with a thioredoxin-like fold comprised of three helices and four sheets in a $\beta\alpha\beta\alpha\beta\alpha$ run. The binding of glutathione is done in an extended conformation at one end of the four strands of the G-site and it is anchored to the domain through electrostatic interactions.

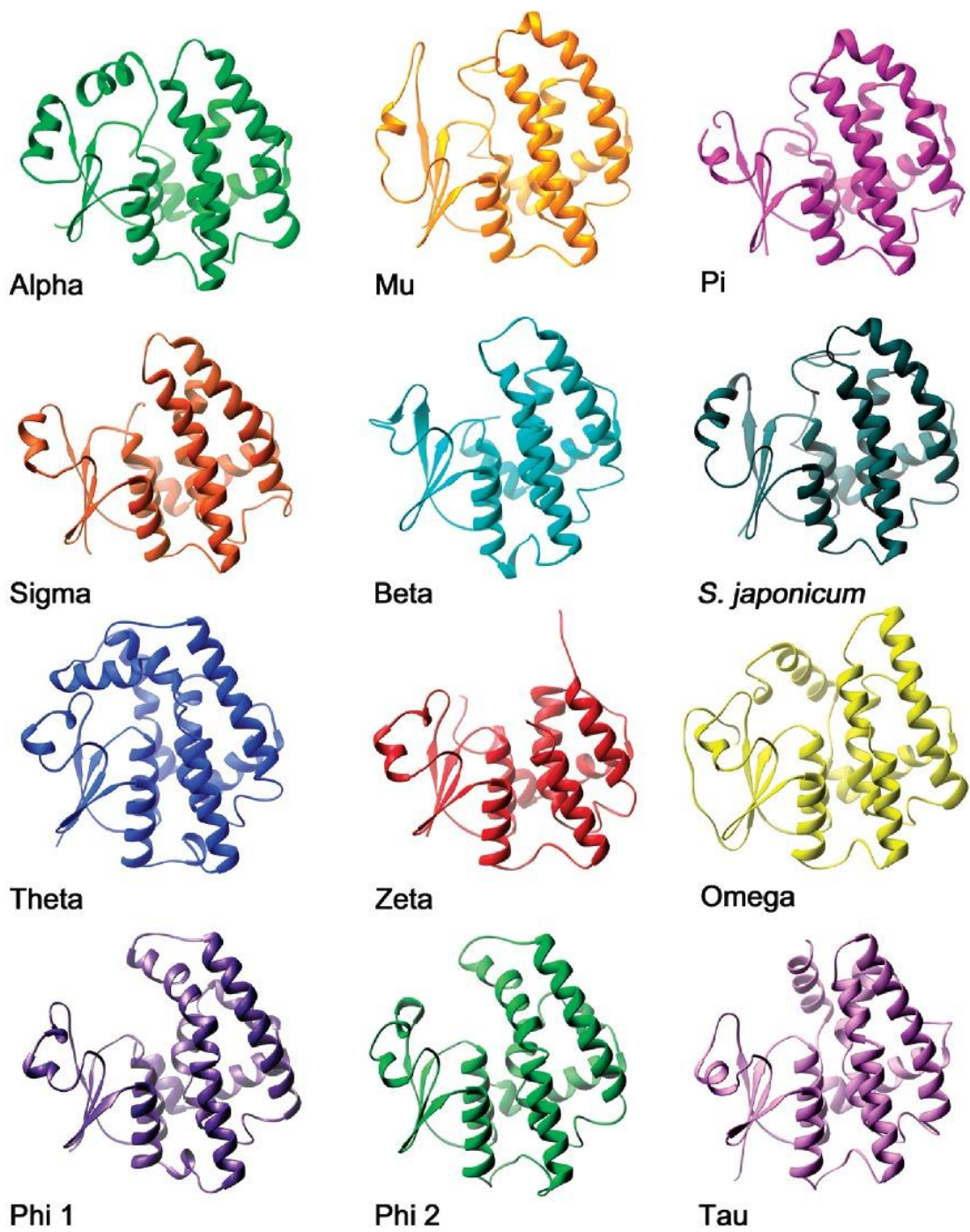


FIGURE 1.3. Three-dimensional structure of the main glutathione transferase monomers (58).

The second domain contains the H-site, *i.e.*, the site for binding of the second, often hydrophobic, substrate. The amino acid residues that are involved in the binding of the electrophilic substrate may also, if correctly positioned, contribute to the chemical steps on the reaction pathway. In any case, the structure of the H-site governs the substrate specificity of a GST. Interestingly, these enzymes have activity only as dimers (Fig. 1.4).

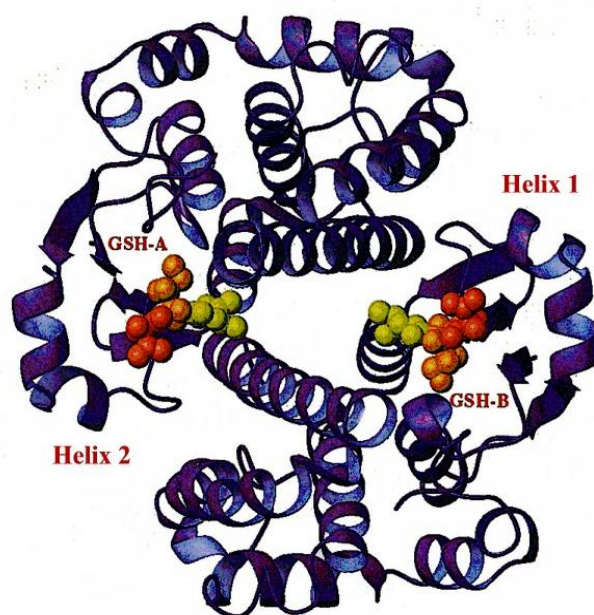


FIGURE 1.4. The homodimer of GSTP1-1 (59).

The argument used to explain this behavior has been the cooperativity (positive or negative) between subunits, recently demonstrated in *Plasmodium falciparum* and some subclasses of mammals isoenzymes in which the subunits showed interactions which modulate the binding of different compounds (60-62). In general, GSTs monomers have molecular masses of 23–28 kDa with an average of 220 amino acids in their sequences. The dimer may have identical subunits (homodimer) or different subunits (heterodimer) of the same class.

The three-dimensional structures of members of mammalian GSTs from classes Alpha (63, 64), Mu (65-66) and Pi (67-69) and mutational studies have provided

important details about amino acid residues putatively involved in the catalytic mechanism. Activation of GSH occurs at the G-site by different amino acids according to the class. Tyrosine (Mu, Pi, Alpha, and Sigma classes), serine (Zeta class) or cysteine (Omega class) allow conjugation or the thiol transfer. The first two amino acids, tyrosine and serine, promote the formation and stabilization of the thiolate anion of GSH, lowering its pK_a from 9.0 to 6.2. This is achieved through hydrogen bond donation of their hydroxyl group, which gets GSH ready for conjugation. When a Cys residue is used there is a thiol transfer, and it forms mixed disulphides with GSH. This kind of reaction is closely related to redox reactions.

The second domain, called the H-site, binds hydrophobic substrates, is located in the C-terminal region and is comprised exclusively of α -helices. The number of the helices varies from 4 to 7. This fact and residue variations in the H-site have been taken as arguments for the wide substrate diversity and preferences for detoxification among classes. For example, the Mu class has very efficient catalysis with molecules containing oxiranes and unsaturated carbonyl groups whereas class Alpha acts on 4-hydroxyalkenals and peroxides (4, 51, 70). However, the subclasses might also be distinguished by their substrate specificities.

1.7.2 GST of human malarial parasites (*Plasmodium falciparum*)

Structures for parasite cytosolic GSTs come from the protozoa *Plasmodium falciparum* (*PfGST*), the nematode *Onchocerca volvulus* (*OvGST2*) and trematodes *Schistosoma haematobium*, *Schistosoma japonicum*, *Schistosoma mansoni* and *Fasciola hepatica*. In all cases, the differences with human cytosolic GSTs provide opportunities to develop specific inhibitors against these parasites (71-76). The GST gene of *Plasmodium falciparum* (*PfGST*) was cloned and expressed in *Escherichia coli*, yielding a homodimeric active enzyme. According to primary structure and substrate specificity, the protein can be placed into the vicinity of the Mu or Pi subclass of GSTs (40). *PfGST* is the only enzyme of the GST family, which in the absence of GSH shows a tetrameric structure rather than a dimeric structure (77).

The structure of *PfGST* at 1.9 and 2.2Å resolution exhibits a shorter C-terminal section, with only five residues after the 8 helix, which implicates a more solvent-accessible H-site area and an amphiphilic character that is reflected in its

substrate spectrum. Amphiphilic compounds, including inhibitors, can access the H-site of *Pf*GST but cannot enter the hydrophobic H-site of human isoforms. Alignments of the *Pf*GST structures with crystals of human Alpha, Mu and Pi classes indicate a significantly high root mean-square (rms; relative position between two atoms) deviation of $\sim 1.2 \text{ \AA}$, compared to members within classes which show rms deviations of $\sim 0.7 \text{ \AA}$, as occurs between *S. japonicum* and *F. hepatica*, which have an rms deviation of 0.85 \AA (27, 72, 75). Again, a broader and more solvent-exposed site is found and it is due to amino acid variation in the H-site of the parasite cytosolic GST in contrast to mammalian Pi class (74). X-ray study of this enzyme, showed by an atypic extra loop connecting helix 4 and helix 5 (residues 113-118) that could be involved in the dimer/dimer interaction. Actually, in the absence of ligands two biological dimers (AA1 and BB1) form a tetramer and these homodimers (Fig. 1.5) are interlocked with each other by the loop 113-118 of monomer B (B1), which occupies the H-site of monomer A (A1) (50).

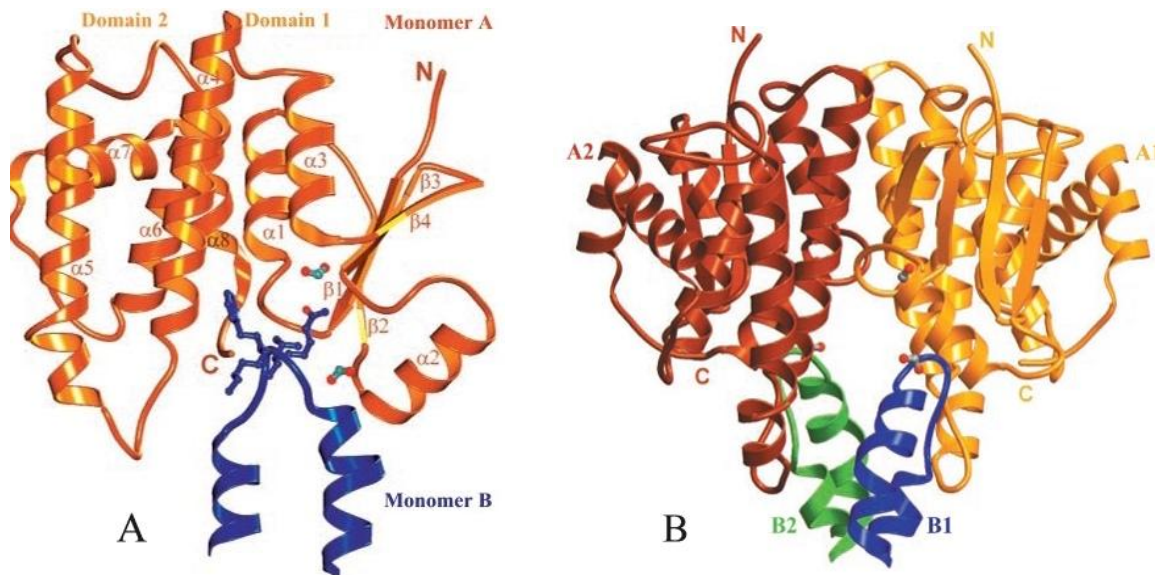


FIGURE 1.5. Structure of the *Pf*GST. (A), dimer structure, (B), tetramer structure (50).

Upon binding of S-hexylglutathione, the H-site loop 113-118 rearranges, residues Asn-114, Leu-115, and Phe-116 form an additional coil in helix α -4 and the side chains of Asn-111, Phe-116, and Tyr-211 flip into the H-site. The changed course of the residues 113-120 in the liganded enzyme prevents the interlocking of the dimers; as a consequence, the molecules are packed as dimers (78).

1.8 GSTs and Nitric Oxide

1.8.1 Nitric oxide (Nitrogen monoxide)

Nitric oxide (NO) is a paramagnetic inorganic gas with good solubility in water, weakly polar and thermodynamically unstable (79). NO is produced in bodies from endogenous and exogenous sources. In the second case, it is synthesized by the enzyme nitric oxide synthase (NOS) in which L-arginine is converted into NO and L-citrulline (80, 81). There are three NOS isoforms: neuronal NOS (nNOS, NOS-1), inducible NOS (iNOS, NOS-2), and endothelial NOS (eNOS, NOS-3) (81). All mammalian NOS are hemoproteins, require NADPH and O₂ for the production of NO, and use FAD, FMN, and tetrahydrobiopterin as cofactors (81-83).

NO is an important molecule involved in a wide range of physiological functions as control of blood pressure, vasodilatation, inhibition of platelet aggregation, neurotransmission, memory formation, penile erection. Furthermore NO is involved in the operation of the immune system, iron metabolism and contributes to the cytotoxicity of activated macrophages against tumor cells and intracellular parasites (84-88). Nitric oxide is reported to induce apoptosis and initiate differentiation in certain types of cancer cells, suggesting that NO is a potential cancer therapeutic agent with novel mechanisms of action (89-91). Furthermore endogenously synthesized NO has been implicated as being responsible for the development of various diseases (92-94). Although the precise mechanisms of biological action of nitric oxide are not completely elucidated, the physiological effects of nitric oxide are dependent on its local concentration and duration of exposure (95, 96).

The most important biological reactions of NO are with oxygen, superoxide and metal ions (97). NO is an odd electron species with a half-life of only a few seconds in biological systems (98) and it reacts rapidly with superoxide to form the cytotoxic peroxynitrite (ONOO^-) (99). It degrades rapidly to nitrite (NO_2^-) then nitrate (NO_3^-) (79, 100, 101). Putative intermediate metabolites include an array of low and high molecular weight compounds, including nitrosogluthathione, nitrosoalbumin, and S-nitrosohaemoglobin (102-104). The presence of a single electron in the NO molecule gives it a radical character and therefore, high reactivity. Between its reactions, NO can lose an electron forming nitrosylic compounds, of mostly covalent character, or to coordinate with variety of metals forming metal-nitrosyl compounds (105).

1.8.2 Dinitrosyl iron complex

All biological activities of nitric oxide can be affected not only by NO itself but also by relatively stable physiological NO carriers or NO donors among which S-nitrosothiol (RSNO) and dinitrosyl iron complexes (DNICs) are included (79, 106). DNICs are stable paramagnetic molecules that exhibits a characteristic spectrum of electron paramagnetic resonance (EPR) (107-110). It is generated in cells and tissues from various sources following exposure to endogenous or exogenous NO and can be detected by EPR spectroscopy (111-119). Mononuclear dinitrosyl iron complexes are formed when ferrous iron and NO react with low molecular weight thiols (120) amino acids, peptides and various proteins (110). In mammalian tissues and cells, the first detection of DNIC derived EPR signals ($g = 2.03$), has been reported more than 30 years ago by Vanin *et al.* (108).

In vivo, dinitrosyl-diglutathionyl iron complex (DNDGIC) and other low mass DNICs could be in equilibrium with several protein-bound forms after replacing one or both the free thiol ligands with protein residues like His, Cys and Ser (121). Both low mass and high mass DNICs seem to be more stable than NO and may possibly act as storage of nitric oxide (122-124) as well as intermediates in the iron-catalyzed formation and decomposition of S-nitrosothiols (125). DNICs can cross cell membranes to donate Fe to tissues (126) and can transnitrosylate acceptor targets *in vitro* and *in vivo* (125, 127, 128) demonstrating their bioavailability and

potential role as NO carrier molecules. DNICs also inhibit platelet aggregation (129), reduce blood pressure (130), relax vascular vessels (131), induce accumulation of heat shock protein Hsp70 (132, 133), and modulate ion channel activity (134).

Up to a few years ago no relation had been found between GSTs and the NO carriers like DNICs, but in 2001 Ricci and co-workers have described the peculiar interaction between of DNDGIC (Fig. 1.6) with GSTP1-1, a representative member of the human glutathione transferase superfamily (135).

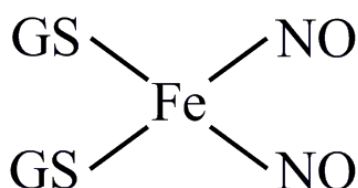


FIGURE 1.6. Dinitrosyl-diglutathionyl iron complex (DNDGIC).

The study of the interaction of DNDGIC with GSTP1-1 demonstrated that this complex is a potent natural competitive inhibitor of this enzyme (135). EPR spectroscopy and molecular modeling indicated that DNDGIC is stabilized in the G-site through the usual polar and hydrophobic interactions of protein residues with one GSH molecule, coordination of the iron ion to the hydroxyl group of Tyr-7, and additional van der Waals interactions of NO moieties with Ile-104 and Tyr-108 (135). This was later confirmed by the crystal structure (136).

More recently Ricci and co-workers demonstrated that not only GSTP1-1 but representative members of all mammalian GSTs interact with DNDGIC showing similar binding mechanism and cooperativity (137). This complex binds with extraordinary affinity to the active site of all GSTs (dimeric enzymes); GSTA1-1 shows the strongest interaction ($K_D \approx 10^{-10}$ M), whereas GSTM2-2 and GSTP1-1 display similar and slightly lower affinities ($K_D \approx 10^{-9}$ M). Binding of the DNDGIC to GSTA1-1 triggers structural intersubunit communication, which lowers the affinity for DNDGIC in the vacant subunit and also causes a drastic loss of enzyme activity. Negative cooperativity is also found in GSTM2-2 and GSTP1-1, but it does

not affect the catalytic competence of the second subunit (137). The EPR spectrum of the GST-bound dinitrosyl iron complexes changes appreciably according to the GST isoform used (Fig. 1.7). The A1-1 and M2-2 classes of GSTs give essentially axial spectra, whereas P1-1 and T2-2 give strongly rhombic spectra, but there are minor differences in the spectra that in practice make it possible to identify the type of glutathione transferase involved directly from the EPR spectrum.

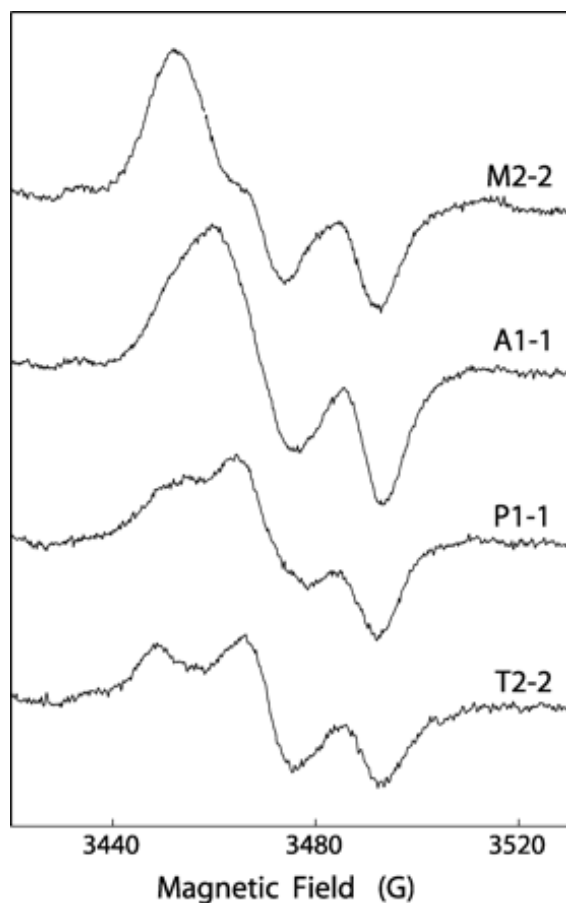


FIGURE 1.7. EPR spectra of DNDGIC bound to different GST isoforms (137).

All these findings suggest a new and important role of GSTs in the metabolism of NO in the cell that may disclose interesting scenarios of research.

The dinitrosyl iron complex is firmly bound to these GST isoforms through the glutathione thiolate-iron-tyrosinate ligand arrangement; constant S-Fe-O bond angles and bond lengths are essential for the high affinity, whereas the positions of the NO groups, which do not seem to contribute much to binding, will be determined by the space available in the active site of the enzyme (137).

1.9 References

1. Sheehan, D., Meade, G., Foley, V. M., and Dowd, C. A. (2001) *Biochem. J.* **360**, 1-16
2. Keen, J. H., and Jakoby, W. B. (1978) *J. Biol. Chem.* **253**, 5654-5657
3. Hayes, J. D., and Pulford, D. J. (1995) *Crit. Rev. Biochem. Mol. Biol.* **30**, 445-600
4. Armstrong, R. N. (1997) *Chem. Res. Toxicol.* **10**, 2-18
5. Hayes, J. D., and McLellan, L. I. (1999) *Free Radic. Res.* **31**, 273-300
6. Laughlin, L. T., Bernat, B. A., and Armstrong, R. N. (1998) *Chem. Biol. Interact.* **111-112**, 41-50
7. Pemble, S. E., Wardle, A. F., and Taylor, J. B. (1996) *Biochem. J.* **319**, 749-754
8. Awasthi, Y. C., Sharma, R., and Singhal, S. S. (1994) *Int. J. Biochem.* **26**, 295-308
9. Sugimoto, M. (1995) *Nippon Rinsho* **53**, 1253-1259
10. Ladner, J. E., Parsons, J. F., Rife, C. L., Gilliland, G. L., and Armstrong, R. N. (2004) *Biochem. J.* **43**, 352-361
11. Robinson, A., Huttley, G. A., Booth, H. S., and Board, P. G. (2004). *Biochem. J.* **379**, 541-552
12. Jakobsson, P. J., Morgenstern, R., Mancini, J., Ford-Hutchinson, A., and Persson, B. (1999) *Protein Sci.* **8**, 689-669
13. Alias, Z., and Clark, A. G. (2007) *Proteomics* **7**, 3618-3628
14. Dixon, D. P., Davis, B. G., and Edwards, R. (2002) *J. Biol. Chem.* **277**, 30859-30869
15. Allocati, N., Favaloro, B., Masulli, M., Alexeyev, M. F., and Di Ilio, C. (2002) *Biochem. J.* **373**, 305-311
16. Wiktelius, E., and Stenberg, G. (2007) *Biochem. J.* **406**, 115-123
17. Mannervik, B. (1985) *Adv. Enzymol. Relat. Areas. Mol. Biol.* **57**, 357- 417
18. Dreij, K., Sundberg, K., Johansson, A. S., Seidel, E., Persson, B., Mannervik, B., and Jernstrom, B. (2002) *Chem. Res. Toxicol.* **15**, 825-831

19. Bruns, C. M., Hubatsch, I., Ridderstrom, M., Mannervik, B., and Tanner, J. A. (1999) *J. Mol. Biol.* **288**, 427-439
20. Nilsson, L. O., Gustaffson, A., and Mannervik, B. (2000) *Proc. Natl. Acad. Sci. U. S. A.* **97**, 9408-9412
21. Hurst, R., Bao, Y., Jemth, P., Mannervik, B., and Williamson, G. (1998) *Biochem. J.* **332**, 97-100
22. Zhao, T., Singhal, S. S., Piper, J. T., Cheng, J., Pandya, U., Clark-Wronski, J., Awasthi, S., and Awasthi, Y. C. (1999) *Arch. Biochem. Biophys.* **367**, 216-224
23. Tetlow, N., Coggan, M., Casarotto, M. G., Board P. G. (2004) *Pharmacogenetics* **14**, 657-663
24. Agosin, M., Naquira, C., Capdevila, J., and Pulin, J. (1976) *Int. J. Biochem.* **7**, 585-593
25. Precious, W., and Barret, J. (1989) *Biochem. Biophys. Acta* **992**, 215-222
26. Tracy, J. W., and Vande Waa, E. A. (1995) *Biochemistry and Molecular Biology of Parasites*. pp. 161-173, Academic Press, San Diego
27. Deponte, M., and Becker, K. (2005) *Methods Enzymol.* **401**, 240-252
28. Barrett, J. (1998) *Comp. Biochem. Physiol.* **121**, 181-183
29. Brophy, P. M., and Pritchard, D. I. (1994) *Exp. Parasitol.* **79**, 89-99
30. Snow, R. W., Guerra, C. A., Noor, A. M., Myint, H. Y., and Hay, S. I. (2005) *Nature* **434**, 214-217
31. Sachs, J., and Malaney, P. (2002) *Nature* **415**, 680-685
32. Olliaro, P. (2001) *Pharmacol. Ther.* **89**, 207-219
33. Greenwood, B., and Mutabingwa, T. (2002) *Nature* **415**, 670-672
34. Ridley, R. G. (2002) *Nature* **415**, 686-693
35. Bannister, L. H., Hopkins, J. M., Fowler, R. E., Krishna S., and Mitchell, G. H. (2000) *Parasitol. Today* **16**, 427-433
36. Krugliak, M., Zhang F., and Ginsburg, H. (2002) *Mol. Biochem. Parasitol.* **119**, 249-256

37. Egan, T. J., Combrinck, J. M., Egan, J., Hearne, G. R., Marques, H. M., Ntenteni, S., Sewell, B. T., Smith, P. J., Taylor, D., van Schalkwyk, D. A., and Walden, J. C. (2002) *Biochem. J.* **365**, 343-347
38. Pagola, S., Stephens, P. W., Bohle, D. S., Kosar A. D., and Madsen, S. K. (2000) *Nature* **404**, 307-310
39. Harwaldt, P., Rahlfs, S., and Becker, K. (2002) *Biol. Chem.* **383**, 821-830
40. Liebau, E., Bergmann, B., Campbell, A. M., Teesdale-Spittle, P., Brophy, P. M., Luersen, K., and Walter, R. D. (2002) *Mol. Biochem. Parasitol.* **124**, 85-90
41. Mannervik, B., and Danielson, U. H. (1988) *CRC Crit. Rev. Biochem.* **23**, 283-337
42. Chemale, G., Morphew, R., Moxon, J. V., Morassuti, A. L., Lacourse, E. J., Barrett, J., Johnston, D. A., and Brophy, P. M. (2006) *Proteomics* **6**, 6263-6273
43. Girardini, J., Amirante, A., Zemzoumi, K., and Serra, E. (2002) *Eur. J. Biochem.* **269**, 5512-5521
44. Hong, S., Lee, J., Lee, D., Sohn, W., and Cho, S. (2001) *Mol. Biochem. Parasitol.* **115**, 69-75
45. Kang, S., Ahn, I., Park, C., Chung, Y., Hong, S., Kong, Y., Cho, S., and Hong, S. (2001) *Exp. Parasitol.* **97**, 186-195
46. Rathaur, S., Fisher, P., Domagalski, M., Walter, R. D., and Liebau, E. (2003) *Exp. Parasitol.* **103**, 177-181
47. Salinas, G., Braun, G., and Taylor, D. W. (1994) *Mol. Biochem. Parasitol.* **66**, 1-9
48. Salvatore, L., Wijffels, G., Sexton, J., Panaccio, M., Mailer, S., McCauley, I., and Spithill, T. (1995) *Mol. Biochem. Parasitol.* **69**, 281-288
49. Vibanco-Pérez, N., Jiménez, L., Mendoza-Hernández, G., and Landa, A., (2002) *Parasitol. Res.* **88**, 398-404
50. Fritz-Wolf, K., Becker, A., Rahlfs, S., Harwaldt, P., Schirmer, R.H., Kabsch, W., and Becker, K. (2003) *Proc. Natl. Acad. Sci. U. S. A.* **100**, 13821-13826

51. Hayes, J. D., Flanagan, J. U., and Jowsey, I. R. (2005) *Annu. Rev. Pharmacol. Toxicol.* **45**, 51-88
52. Wilce, M. C., and Parker, M. W. (1994) *Biochim. Biophys. Acta* **1205**, 1-18
53. Pickett, C. B., and Lu, A. Y. (1989) *Annu. Rev. Biochem.* **58**, 743-764
54. Ketterer, B., Fraser, G., and Meyer, D. J. (1990) *Adv. Exp. Med. Biol.* **264**, 301-310
55. Meyer, D. J., Crease, D. J., and Ketterer, B. (1995) *Biochem. J.* **306**, 565-569
56. Graminski, G. F., Kubo, Y., and Armstrong, R. N. (1989) *Biochemistry* **28**, 3562-3568
57. Adler, V., Yin, Z., Fuchs, S. Y., Benezra, M., Rosario, L., Tew, K. D., Pincus, M. R., Ardana, M., Henderson, C. J., Wolf, C. R., Davis, R. J., and Ronai, Z. (1999) *EMBO J.* **18**, 1321-1334
58. Thomas, D. D., Liu, X., Kantrow, S. P., and Lancaster, J. R. (2001) *Proc. Natl. Acad. Sci. U. S. A.* **98**, 355-360
59. Oakley, A. J., Lo Bello, M., Mazzetti, A. P., Federici, G., and Parker, M. W. (1997) *FEBS Lett.* **419**, 32-36
60. Ricci, G., Turella, P., De Maria, F., Antonini, G., Nardocci, L., Board, P. G., Parker, M. W., Carbonelli, M. G., Federici, G., and Caccuria, A. M. (2004) *J. Biol. Chem.* **279**, 33336-33342
61. Armstrong, R.N. (1994) *Adv. Enzymol.* **69**, 1-44
62. Liebau, E., De Maria, F., Burmeister, C., Perbandt, M., Turella, P., Antonini, G., Federici, G., Giansanti, F., Stella, L., Lo Bello, M., Caccuri, A. M., and Ricci, G. (2005) *J. Biol. Chem.* **280**, 26121-26128
63. Sinning, I., Kleywegt, G. J., Cowan, S. W., Reinemer, P., Dirr, H. W., Huber, R., Gilliland, G. L., Armstrong, R. N., Ji, X., Board, P. G., Olin, B., Mannervik, B., and Jones, T. A. (1993) *J. Mol. Biol.* **232**, 192-212
64. Cameron A. D., Sinning, I., L'Hermite, G., Olin, B., Board, P. G., Mannervik, B., and Jones, T. A. (1995) *Structure* **3**, 717-727
65. Ji, X., Zhang, P., Armstrong, R. N., and Gilliland, G. L. (1992) *Biochemistry* **31**, 10169-10184

66. Raghunathan, S., Chandross, R. J., Kretsinger, R. H., Allison, T. J., Penington, C. J., and Rule G. S. (1994) *J. Mol. Biol.* **238**, 815-832
67. Reinemer, P., Dirr, H. W., Ladenstein, R., Schäffer, J., Gallay, O., and Huber, R. (1991) *EMBO J.* **10**, 1997-2005
68. Reinemer, P., Dirr, HW., Ladenstein, R., Huber, R., Lo Bello, M., Federici, G., and Parker, M. W. (1992) *J. Mol. Biol.* **227**, 4-26
69. Dirr, H., Reinemer, P., and Huber, R. (1994) *J. Mol. Biol.* **243**, 72-92
70. Frova, C. (2006) *Biomol. Eng.* **23**, 149-169
71. Baiocco, P., Gourlay, L. J., Angelucci, F., Fontaine, J., Hervé, M., Miele, A. E., Trottein, F., Brunori, M., and Bellelli, A. (2006) *J. Mol. Biol.* **360**, 678-689
72. Burmeister, C., Perbandt, M., Betzel, C., Walter, R. D., and Liebau, E. (2003) *Acta Crystallogr. D Biol. Crystallogr.* **59**, 1469-1471
73. McTigue, M., Williams, D. R., and Tainer, J. A., (1995) *J. Mol. Biol.* **246**, 21-27
74. Perbandt, M., Höppner, J., Betzel, C., Walter, R. D., and Liebau, E. (2005) *J. Biol. Chem.* **280**, 12630-12636
75. Rossjohn, J., Feil, S. C., Wilce, M. C. J., Sexton, J. L., Spithill, T. W., and Parker, M. W. (1997) *J. Mol. Biol.* **273**, 857-872
76. Trottein, F., Vaney, M. C., Bachet, B., Pierce, R. J., Colloch, N., Lecocq, J. P., Capron, A., and Mornon, J. P. (1992) *J. Mol. Biol.* **224**, 515-518
77. Tripathi, T., Rahlfs, S., Becker, K., and Bhakuni, V. (2007) *BMC Struct Biol.* **7**, 67
78. Hiller, N., Fritz-Wolf, K., Deponte, M., Wende, W., Zimmermann, H., and Becker, K. (2006) *Protein* **15**, 281-289
79. Butler, A. R., and Williams, D. L. H. (1993) *Chem. Soc. Rev.* **22**, 233-241
80. Stuehr, D. J., and Griffith, O. W. (1992) *Advances in enzymology and related areas of molecular biology*. pp. 287-346, John Wiley & Sons, New York
81. Morris, S. M. Jr. (2005) *Vasc. Med.* **10**, 83-87
82. Knowles, R. G., and Moncada, S. (1994) *Biochem. J.* **298**, 249-258
83. White, K. A., and Marletta, M. A. (1992) *Biochem. J.* **31**, 6627-6631

84. Moncada, S. J. (1994) *Hypertens. Suppl.* **12**, 35-39
85. Loscalzo, J., and Welch, G. (1995) *Prog. Cardiovasc. Dis.* **38**, 87-104
86. Nathan, C. (1992) *FASEB J.* **6**, 3051-3064
87. Stamler, J. S. (1994) *Cell* **78**, 931-936
88. Thippeswamy, T., McKay, J. S., Quinn, J. P., and Morris, R. (2006) *Histol. Histopathol.* **21**, 445-458
89. Magrinat, G., Mason, S. N., Shami, P. J., and Weinberg, J. B. (1992) *Blood* **80**, 1880-1884
90. Shami, P. J., Moore, J. O., Gockerman, J. P., Hathorn, J. W., Misukonis, M. A., and Weinberg, J. B. (1995) *Leukemia Res.* **19**, 527-533
91. Shami, P. J., Sauls, D. L., and Weinberg, J. B. (1998) *Leukemia* **12**, 1461-1466
92. Moncada, S., Palmer, R. M., and Higgs, E. A. (1991) *Pharmacol. Rev.* **43**, 109-142
93. Tamir, S., and Tannenbaum, S. R. (1996) *Biochim. Biophys. Acta* **1288**, 31-36
94. Mey, C. (1998) *Curr. Med. Res. Opin.* **14**, 187-202
95. Wink, D. A., and Mitchell, J. B. (2003) *Free Rad. Biol. Med.* **34**, 951-954
96. Wink, D. A., Vodovotz, Y., Laval, J., Laval, F., Dewhirst, M. W., and Mitchell, J. B. (1998) *Carcinogenesis* **19**, 711-721
97. Stamler, J. S., Singel, D. J., and Loscalzo, J. (1992) *Science* **258**, 1898-1902
98. Thomas, D. D., Liu, X., Kantrow, S. P., and Lancaster, J. R., Jr. (2001) *Proc. Natl. Acad. Sci. U. S. A.* **98**, 355-360
99. Beckman, J. S., Beckman, T. W., Chen, J., Marshall, P. A., and Freeman, B. A. (1990) *Proc. Natl. Acad. Sci. U. S. A.* **87**, 1620-1624
100. Lam, A. A., Hyland, K., and Heales, S. J. (2007) *J. Inherit. Metab. Dis.* **30**, 256-622
101. Lancaster, J. R., (1994) *Proc. Natl. Acad. Sci. U. S. A.* **91**, 8137-8141
102. Kukovetz, W. R., Holzmann, S., and Schmidt, K. (1991). *Eur. Heart J.* **12**, 1-24
103. Marks, D. S., Vita, J. A., Folts, J. D., Keaney, J. F., Welch, G. N., and Loscalzo, J. (1995) *J. Clin. Invest.* **96**, 2630-2638

104. Jia, L., Bonaventura, C., Bonaventura, J., and Stamler, J. S. (1996) *Nature* **380**, 221-226
105. Xu, W. M. and Liu, L. Z. (1998) *Cell Res.* **8**, 251-258
106. Henry, Y., Lepoivre, M., Ducrocq, C., Boucher J. L., and Guissani A. (1993) *FASEB J.* **7**, 1124-1134
107. Vithayathil, A. J., Ternberg, J. L., and Commoner, B. (1965) *Nature* **207**, 1246-1249
108. Vanin, A. F., and Nalbandian R. M. (1965) *Biofizika* **10**, 167-168
109. Vanin, A. F., Bliumenfel'd, L. A., and Chetverikov, A.G. (1967) *Biofizika* **12**, 828-848
110. Woolum, J. C., Tiezzi, E., and Commoner, B. (1968) *Biochim. Biophys. Acta* **160**, 311-320
111. Woolum, J. C., and Commoner, B. (1970) *Biochim. Biophys. Acta* **201**, 131-135
112. Chiang, R. W., Woolum, J. C., and Commoner, B. (1972) *Biochim. Biophys. Acta* **257**, 452-460
113. Reddy, D., Lancaster, J. R., and Cornforth, D. P. (1983) *Science* **221**, 769-770
114. Drapier, J. C., Pellat, C., and Henry, Y. (1991) *J. Biol. Chem.* **266**, 10162-10167
115. Lancaster, J. R., Langrehr, J. M., Bergonia, H. A., Murase, N., Simmons, R. L., and Hoffman, R. A. (1992) *J. Biol. Chem.* **267**, 10994-10998
116. Stadler, J., Bergonia, H. A., Di Silvio, M., Sweetland, M. A., Billiar, T. R., Simmons, R. L., and Lancaster, J. R. (1993) *Arch. Biochem. Biophys.* **302**, 4-11
117. Vanin, A. F., Mordvintcev, P. I., Hauschildt, S., and Mülsch, A. (1993) *Biochim. Biophys. Acta* **1177**, 37-42
118. Bastian, N. R., Yim, C. Y., Hibbs, J. B., and Samlowski, W. E. (1994) *J. Biol. Chem.* **269**, 5127-5131.
119. Lancaster, J. R., Werner-Felmayer, G., and Wachter, H. (1994) *Free Radic. Biol. Med.* **16**, 869-870

120. McDonald, C. C., Phillips, W. D., and Mower, H. F. (1965) *J. Am. Chem. Soc.* **87**, 3319-3326
121. Ueno, T., and Yoshimura, T. (2000) *Jpn J. Pharmacol.* **82**, 95-101
122. Mülsch, A., Mordvintcev, P., Vanin, A. F., and Büsse, R. (1991) *FEBS Lett.* **294**, 252-256
123. Mülsch, A., Mordvintcev, P. I., Vanin, A. F., Busse, R. (1993) *Biochem. Biophys. Res. Commun.* **196**, 1303-1308
124. Muller, B., Kleschyov, A. L., and Stoclet, J. C. (1996) *Br. J. Pharmacol.* **119**, 1281-1285
125. Vanin, A. F., Malenkova, I. V., and Serezhenkov, V. A. (1997) *Nitric Oxide* **1**, 191-203
126. Ueno, T., Suzuki, Y., Fujii, S., Vanin, A. F., and Yoshimura, T. (1999) *Free Radic. Res.* **31**, 525-534
127. Ueno, T., Suzuki, Y., Fujii, S., Vanin, A. F., and Yoshimura, T. (2002) *Biochem. Pharmacol.* **63**, 485-493
128. Boese, M., Mordvintcev, P. I., Vanin, A. F., Büsse, R., and Mülsch, A. (1995) *J. Biol. Chem.* **270**, 29244-29249
129. Vanin, A. F. (1991) *FEBS Lett.* **289**, 1-3
130. Manukhina, E. B., Malyshev, I. Y., Malenyuk, E. B., Zenina, T. A., Pokidyshev, D. A., Mikojan, V. D., Kubrina, L. N., and Vanin, A. F. (1998) *Biull. Eksp. Biol. Med.* **125**, 30-33
131. Mülsch, A. (1994) *Arzneim. Forsch.* **44**, 408-411
132. Malyshev, I. Y., Malugin, A. V., Golubeva, L. Y., Zenina, T. A., Manukhina, E. B., Mikojan, V. D., and Vanin, A. F. (1996) *FEBS Lett.* **391**, 21-23
133. Malyshev, I. Y., Zenina, T. A., Golubeva, L. Y., Saltykova, V. A., Manukhina, E. B., Mikojan, V. D., Kubrina, L. N., and Vanin, A. F. (1999) *Nitric Oxide* **3**, 105-113
134. Giannone, G., Takeda, K., and Kleyshev, A. L. (2000) *J. Physiol. (Lond.)* **529**, 735-745

135. Lo Bello, M., Nuccetelli, M., Caccuri, A. M., Stella, L., Parker, M. W., Rossjohn, J., McKinstry, W. J., Mozzi, A. F., Federici, G., Polizio, F., Pedersen, J. Z., and Ricci, G. (2001) *J. Biol. Chem.* **276**, 42138-42145
136. De Maria, F., Pedersen, J. Z., Caccuri, A. M., Antonini, G., Turella, P., Stella, L., Lo Bello, M., Federici, G., and Ricci, G. (2003) *J. Biol. Chem.* **278**, 42283-42293
137. Cesareo, E., Parker, L. J., Pedersen J. Z., Nuccetelli, M., Mazzetti, A. P., Pastore, A., Federici, G., Caccuri, A. M., Ricci, G., Julian J., Adams, J. J., Parker, M. W., and Lo Bello, M. (2005) *J. Biol. Chem.* **280**, 42172-42180

AIM OF THESIS

Targets of the present study may be summarized as follows:

1. Study on the interaction of rat liver GSTs with DNDGIC in living cells and tissues. Investigation on the possible physiological roles of this interaction.
2. Study of the subcellular localization of GST in rat hepatocytes. Role of Alpha GSTs as protection enzymes localized near the nuclear envelope.
3. Identification of protein segments in the glutathione transferase from *Plasmodium falciparum* that modulate the peculiar dimer - tetramer transition and the cooperative binding of the parasitotoxic hemin.

**2. STUDY OF THE INTERACTION
BETWEEN GSTs AND DNDGIC IN
INTACT CELLS AND TISSUES**

2.1 Introduction

Dinitrosyl iron complexes (DNICs) are paramagnetic compounds observed in isolated cells or tissues incubated or perfused with NO or NO-generating systems (1-5). Traces are also present in tissues under physiological conditions (4). These complexes, in which ferrous ion coordinates two nitric oxide molecules together with two other ligands, show characteristic EPR spectra centered at about $g = 2.03$ that made possible their discovery in cells or tissues. Although the occurrence of DNICs has been demonstrated unequivocally, their chemical identity *in vivo* is still ambiguous. In fact, they may exist as free low molecular mass complexes of the general formula $(\text{NO})_2(\text{RS})_2\text{Fe}$, *e.g.* the dinitrosyl-diglutathionyl iron complex (DNDGIC) and dinitrosyl-dicysteinylyl iron complex but the existence of such free complexes *in vivo* has never been demonstrated; they always appear bound to unknown proteins (1). The binding to proteins is possible after replacing one thiol ligand of the free complex with a protein serine, tyrosine, or cysteine to complete the coordination shell of the iron. All these paramagnetic species show very similar EPR spectra centered around $g = 2.03$, thus this technique is unable to define their precise chemical composition (6). Also the physiological role of DNICs is controversial; it has been suggested that they function as more stable natural NO carriers, but they are also known to have toxic effects in biological systems (1). In particular, DNDGIC at micromolar concentrations is a potent and irreversible inhibitor of glutathione reductase (7, 8).

It has been proposed that glutathione transferases (GSTs) could be involved in the DNIC binding, storage, and detoxification in living systems (9-11). In fact, we recently demonstrated that Alpha, Pi, and Mu class GSTs, which represent 90-95% of all mammalian GSTs, bind the dinitrosyl-diglutathionyl iron complex with extraordinary high affinity, showing K_D values of 10^{-10} - 10^{-9} M (9-11). The association of DNDGIC to GSTs has been thoroughly investigated, revealing that one of the glutathiones in the iron complex binds to the enzyme G-site, whereas the other GSH molecule is lost and is replaced by a tyrosine phenolate in the coordination of the ferrous ion (11). Thus, the bound complex is a monogluthationyl species (DNGIC). The X-ray crystallographic structure of DNGIC bound to

GSTP1-1 has been solved recently, confirming the structure proposed on the basis of molecular modeling studies (12). Binding of DNGIC to the first subunit of the dimeric Alpha, Pi, and Mu GSTs also triggers a peculiar intersubunit communication, which lowers the affinity of the second subunit (11). We suggested that in crude liver homogenates one target of DNICs could be the pool of GSTs (10), which thus could represent a significant part of the "unknown" proteins that apparently bind DNICs. Furthermore, the intracellular iron source for DNIC formation has never been determined. This study demonstrates that DNDGIC is formed spontaneously in intact rat hepatocytes after exposure to GSNO; this complex is never detected as free species but always bound to GSTs. The preferential binding proteins in rat hepatocytes are the Alpha class GSTs, which stabilize the complex for many hours. Ferritin is the iron source for DNDGIC, but the amount of complex formed never exceeds the buffer capacity of the endogenous pool of GSTs. Evidence is also given that this highly specific interaction is essential to protect glutathione reductase against irreversible inactivation by DNDGIC.

2.2 Experimental Procedures

Materials - Human GSTA1-1, GSTM2-2, GSTP1-1 were expressed in *Escherichia coli* and purified as described previously (13-15). MGST1, the microsomal GST, was a generous gift of Prof. R. Morgenstern. The enzyme concentrations reported in the text for all GSTs refer to the single subunit. Horse spleen ferritin (16% iron) was a Fluka product (Buchs, Switzerland).

Preparation of GSNO - GSNO was prepared as described previously (9). Briefly, a few drops of HCl were added to a solution containing equimolar amounts of GSH and sodium nitrite until pH 1.5 was reached. After standing for 5 min at room temperature, the red GSNO was neutralized with NaOH. GSNO displays an absorption maximum of $750 \text{ M}^{-1} \text{ cm}^{-1}$ at 332 nm and appears to be stable for a few days at room temperature. Appropriate aliquots of freshly synthesized compound were stored at 80°C and used when necessary, after checking their absorbance at 332 nm.

Synthesis of DNDGIC - Dinitrosyl-diglutathionyl-iron complex was synthesized according to the following procedure. Suitable amounts of ferrous ions (FeSO_4 , ranging from 10 to 50 μM) were added to a mixture containing 20 mM GSH and 2 mM GSNO in 0.1 M phosphate buffer, pH 7.4, and 25°C . The synthesis of the complex was completed in the first 15-20 min and gives an extinction coefficient of $3000 \text{ M}^{-1} \text{ cm}^{-1}$ at 403 nm (9).

Preparation of rat liver homogenate - Rat liver homogenate was prepared starting from 10 g of Sprague-Dawley male rat liver washed twice with 200 ml of phosphate-buffered saline. The tissue was homogenized in 100 ml of 0.25 M sucrose and centrifuged at $1000 \times g$ to remove the nuclear fraction. The estimated concentration of the GST pool was 18 μM . Alternatively, the rat liver was homogenized in 30 ml of 0.25 M sucrose to obtain a more concentrated GST medium (56 μM). Hepatocytes were isolated from male Wistar rats (2 months old, 100-120 g) as reported previously (16). Rats were anesthetized by pentobarbital

(50 mg/kg body weight, injected intraperitoneally) before rapid killing by cervical dislocation and subsequent liver dissection. Experiments were carried out in accordance with the ethical guidelines for animal research (Italian Ministry of Health).

Preparation of subcellular fractions - After perfusion with 0.25 M sucrose and heparin to remove blood, livers from male rats (about 10 g) were excised, minced, and homogenized in a Potter-Elvehjem in 0.25 M sucrose and 10 mM potassium phosphate buffer, pH 7.4 (50 ml per 5 g of liver). After a brief centrifugation to remove unbroken cells, the homogenate was incubated with 1 mM GSNO for 2 h and then centrifuged at $1000 \times g$ for 10 min to isolate the nuclear fraction. The nuclear pellet was washed three times with 20 ml of 0.25 M sucrose and 10 mM potassium phosphate buffer, pH 7.4. The collected supernatants were centrifuged at $3,300 \times g$ for 10 min to isolate the mitochondrial fraction. With similar procedures the lysosomal fraction ($16,300 \times g$ for 20 min) and the microsomal pellet ($105,000 \times g$ for 30 min) were isolated. Each fraction was washed three times with 10 volumes of 0.25 M sucrose in 10 mM potassium phosphate buffer, pH 7.4. Each fraction was tested for purity through measurement of the activities of several marker enzymes, typically located in separate cellular compartments as follows: glucose-6-phosphate dehydrogenase for the cytosol, cytochrome oxidase for mitochondria, acid lipase for lysosomes, and glucose-6-phosphatase for microsomes. In addition, the quality of isolated nuclei was examined using electron microscopy (not shown). Cross-contamination in each fraction was below 10%. The nuclear fraction showed less than 2% of cytosol contamination; the mitochondrial fraction contained less than 1% of nuclei as judged by DNA content.

GST activity - GST activity was assayed in 0.1 M potassium phosphate buffer, pH 6.5, in the presence of 10 mM GSH and 1 mM of 1-chloro-2,4-dinitrobenzene at 25°C. The reaction was followed spectrophotometrically at 340 nm where the GSH-2,4-dinitrobenzene adduct absorbs ($\epsilon = 9,600 \text{ M}^{-1} \text{ cm}^{-1}$).

Glutathione reductase activity - Glutathione reductase activity was assayed at 25°C using a solution of 1 mM GSSG and 0.1 mM NADPH in 1 ml (final volume) of 0.1 M potassium phosphate buffer, pH 7.4. The activity was followed spectrophotometrically at 340 nm.

EPR analysis - Samples for EPR experiments were usually prepared using hepatocytes in phosphate-buffered saline or rat liver homogenate in 0.25 M sucrose with DNDGIC added from a freshly made stock solution. EPR measurements were carried out at room temperature with a Bruker ESP300 X-band instrument (Bruker, Karlsruhe, Germany) equipped with a high sensitivity TM_{110} -mode cavity. To optimize instrument sensitivity, spectra were recorded using samples of 80 μ l contained in flat glass capillaries (inner cross-section 5×0.3 mm) (17). Unless otherwise stated, spectra were measured over a 200-G range using 20 milliwatts power, 2.0 G modulation, and a scan time of 42 s; typically 4-40 single scans were accumulated to improve the signal to noise ratio. The EPR signal was quantified by comparison with standard samples containing known concentrations of DNDGIC and GST, as described previously (11). The limit of detection was ~ 2 μ M, and the range was linear up to at least 50 μ M DNGIC-GST.

Glutathione reductase activity - Glutathione reductase activity was assayed at 25°C using a solution of 1 mM GSSG and 0.1 mM NADPH in 1 ml (final volume) of 0.1 M potassium phosphate buffer, pH 7.4. The activity was followed spectrophotometrically at 340 nm.

Calculation of intracellular DNIC concentrations - DNDGIC and DNGIC-GST were determined on the basis of EPR spectra. Calculations of the cytosolic concentration of both DNGIC-GST and GSTs in rat hepatocytes and in rat liver homogenates were made assuming a hepatocyte volume of 8×10^{-12} liters and a cytosol volume corresponding to 56% of the cell volume. The volume of the cytosol is 0.28 ml per g of fresh liver (18). The concentration of the cytosolic GSTs was 0.7 mM.

Theoretical inhibition of the cytosolic GSTs because of DNDGIC binding - An inhibition simulation algorithm has been developed based on the following assumptions. (a) In the male rat liver, Alpha and Mu GSTs are 43 and 56%, respectively (19, 20). These values were confirmed for our male rat liver preparations by means of high pressure liquid chromatography. (b) Specific activities of Alpha and Mu GSTs are 16 and 22 units/mg, respectively. These values are the weighted average of the specific activities of the three major Alpha isoenzymes, *i.e.* GSTA1-1 (18 units/ mg), GSTA2-2 (18 units/mg), and GSTA3-3 (14 units/mg), and of the two major Mu isoenzymes, *i.e.* GSTM1-1 (29 units/mg) and GSTM2-2 (15 units/mg) (21). (c) K_D values for the high and low affinity binding sites of Alpha and Mu GSTs were reported previously (11). (d) Half-site inhibition is operative for the Alpha GSTs, *i.e.* 95% inhibition when the enzyme is half-saturated (11).

Statistics - Results are shown as the mean \pm S.D. of at least three experiments.

2.3 Results

2.3.1 Interaction of GSTs with DNDGIC in rat liver homogenate

Kinetics and EPR experiments were used to verify if in rat liver GST represents the prime protein target for DNDGIC among all the cytosolic proteins. Incubation of variable amounts of DNDGIC in a liver homogenate (56 μM total GSTs) caused instantaneous and concentration-dependent loss of GST activity. By considering the relative levels of Alpha and Mu GSTs, their different affinities for the complex ($K_D = 10^{-10}$ for Alpha class and 10^{-9} M for Mu class) of GSTs (11), and their different specific activities, (see “Experimental Procedures”), it is possible to calculate the extent of this inhibition in case DNDGIC binds stoichiometrically and exclusively to GSTs, assuming that the isoenzyme with higher affinity (Alpha GST) is involved first. As shown in Fig. 2.1, the inhibition calculated corresponds well to that found experimentally.

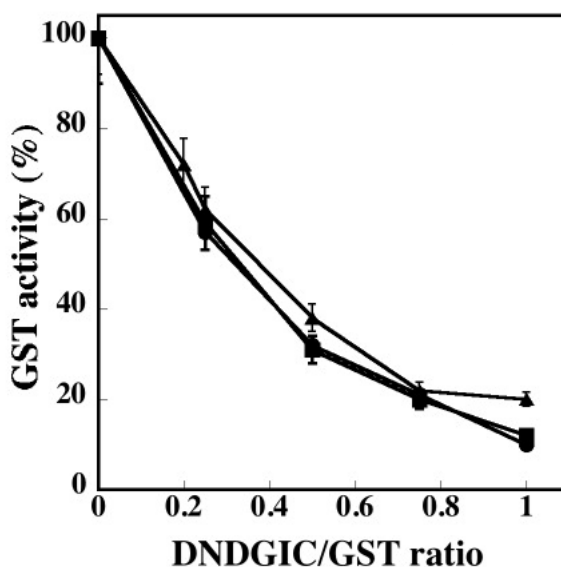


FIGURE 2.1. Inhibition of rat liver GSTs by substoichiometric DNDGIC. ▲, DNDGIC added to a rat liver homogenate (diluted 1:3 in 0.25 M sucrose). Final concentration of GSTs is 28 μM ; ■, DNDGIC added to the purified pool of rat liver GSTs (28 μM final concentration); ●, theoretical inhibition curve for exclusive binding of DNDGIC to GSTs, calculated as reported under “Experimental Procedures.”

The inhibition pattern of the purified pool of liver GSTs is also very similar (Fig. 2.1). As expected, the EPR analysis of the homogenate after reaction with substoichiometric DNDGIC confirmed that all complex is bound to proteins (Fig. 2.2). It should be remembered that in rat liver homogenate the GST-DNGIC signal is stable for many hours, whereas DNDGIC in a GST-depleted homogenate appears as a free species and is highly unstable, with a $t_{1/2}$ of 10 min (10).

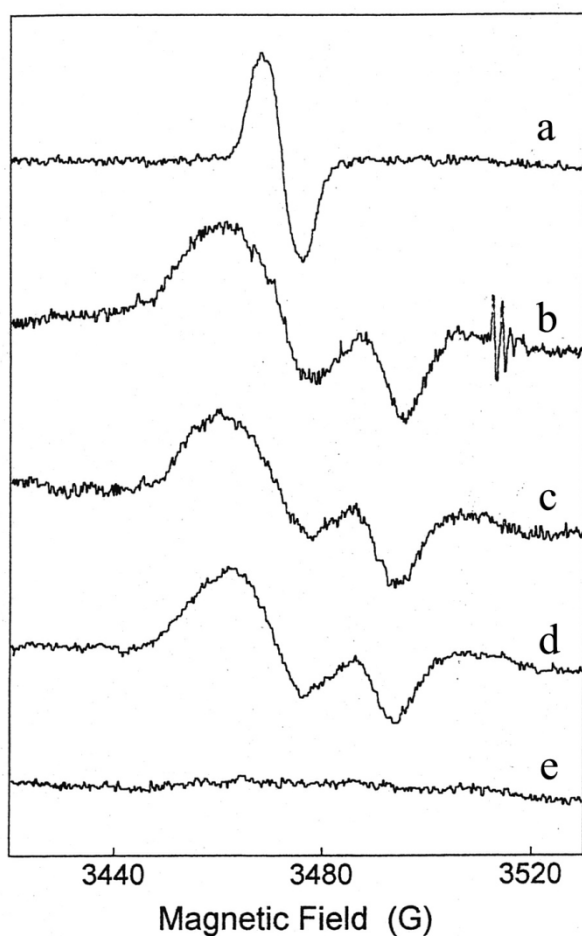


FIGURE 2.2. EPR spectra of DNDGIC and DNGIC-GST. *Spectrum a*, authentic DNDGIC (5 μ M) in 0.1 M potassium phosphate buffer, pH 7.4. *Spectrum b*, DNDGIC (9 μ M) added to a rat liver homogenate containing 18 μ M GSTs. *Spectrum c*, DNDGIC (9 μ M) added to the purified pool of rat liver GSTs (18 μ M) at pH 7.4. *Spectrum d*, DNDGIC (10 μ M) added to purified GSTA1-1 (20 μ M). *Spectrum e*, rat liver homogenate as a control.

2.3.2 Spontaneous formation of DNDGIC by GSNO in rat liver homogenate

When a rat liver homogenate (56 μ M GSTs) depleted only of the nuclear fraction is incubate with 1 mM GSNO, a time-dependent accumulation of DNIC has been observed. The complex reaches an apparent plateau of \sim 18 μ M after two hours of incubation (Fig. 2.3). This is followed by a second phase with a very slow increase that ends only after 14-16 hours, at a concentration of \sim 26 μ M DNIC (not shown).

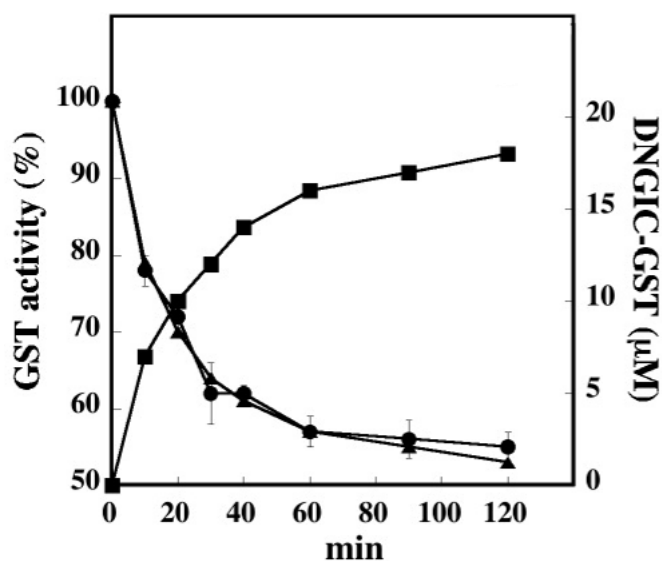


FIGURE 2.3. DNDGIC formation in rat liver homogenate. Rat liver homogenate (diluted 1:3 in 0.25 M sucrose) incubated with 1 mM GSNO at 25°C; ■, DNGIC-GST measured by EPR. ▲, GST activity; ●, theoretical inhibition for an exclusive binding of DNDGIC to GSTs.

The EPR spectra suggest that the iron complex is entirely bound to proteins and that it does not exist as a free species (Fig. 2.4). The EPR spectrum is very similar to that obtained after addition of authentic DNDGIC to the homogenate. The identity of DNGIC-GST confirmed by the GST inhibition pattern that is close to that expected assuming GSTs to be the sole target of this complex (Fig. 2.3). Increasing the final concentration of GSH in the homogenate up to the physiological levels in rat hepatocytes (10 mM) results in faster kinetics of the first phase for DNDGIC formation, but the final amount of complex formed is the same (not shown). The kinetics of DNDGIC formation also depends on GSNO concentration (in the range from 0.2 to 5 mM), but the final concentration of DNGIC-GST does not change appreciably (Fig. 2.5). Thus it appears that iron availability is the limiting factor for the final level of the complex. In our experimental conditions, DNDGIC never exceeds the amount of the endogenous GST pool, which is 56 µM. Only by adding 50 µM of exogenous ferrous ions to the homogenate can the typical EPR signal of unbound DNICs be seen, superimposed on a large GST-DNGIC signal (Fig. 3.4). In that case, the GST activity almost disappears, and the amount of the bound DNIC corresponds to the concentration of the entire pool of cytosolic GSTs.

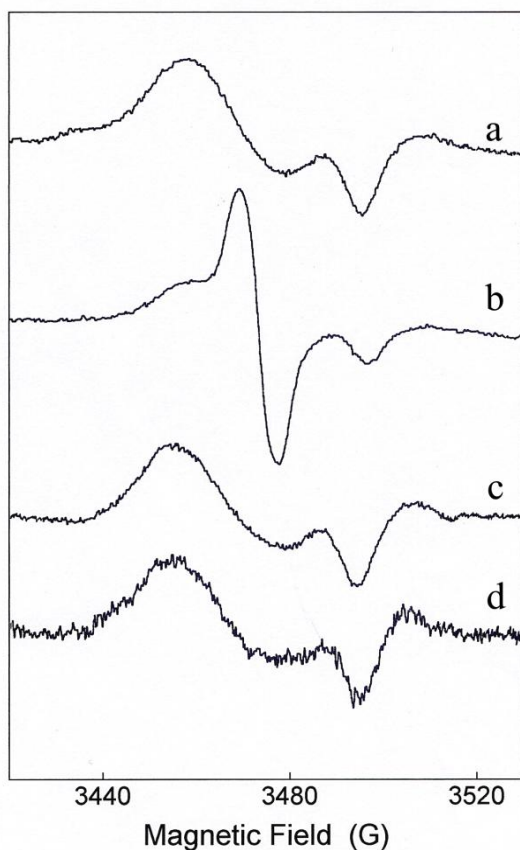


FIGURE 2.4. EPR spectra of DNGIC-GST formed by GSNO. *Spectrum a*, homogenate (56 μM GSTs) after 1 h of incubation with 1mM GSNO. *Spectrum b*, as in a with 50 μM Fe(II) added before incubation; spectrum is shown at half the actual size. *Spectrum c*, hepatocytes (4×10^7 cells) after 1 h of incubation with 1mM GSNO. *Spectrum d*, membrane fraction isolated from sample c; spectrum was amplified twice.

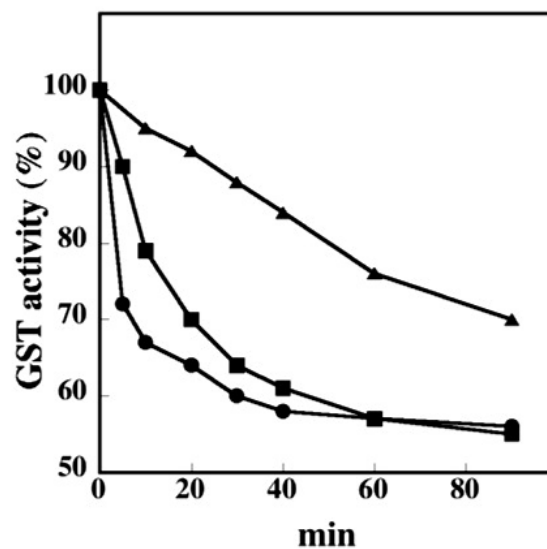


FIGURE 2.5. Dependence of DNGIC-GST formation on GSNO concentration. Variable amounts of GSNO were incubated at 25°C with rat liver homogenate (diluted 1:3 in 0.25 M sucrose). \blacktriangle , 0.2 mM GSNO; \blacksquare , 1mM GSNO; \bullet , 5 mM GSNO.

2.3.3 Formation of DNDGIC in intact rat hepatocytes

Incubation of rat hepatocytes with 1 mM GSNO causes a time-dependent intracellular accumulation of a paramagnetic species with an EPR spectrum centered at $g = 2.03$ very similar to that obtained in the crude homogenate after incubation with GSNO and reasonably due to a DNGIC-GST complex (Fig. 2.4). Also in this case, the kinetics of DNIC formation is proportional to the GSNO concentration (within 0.5 mM and 2 mM) while the final level of the complex is

almost independent (data not shown). After two hours of incubation with 1 mM GSNO, DNGIC-GST reaches a plateau of 12 μM in the sample, corresponding to an intracellular concentration of about 0.19 mM (Fig. 2.6).

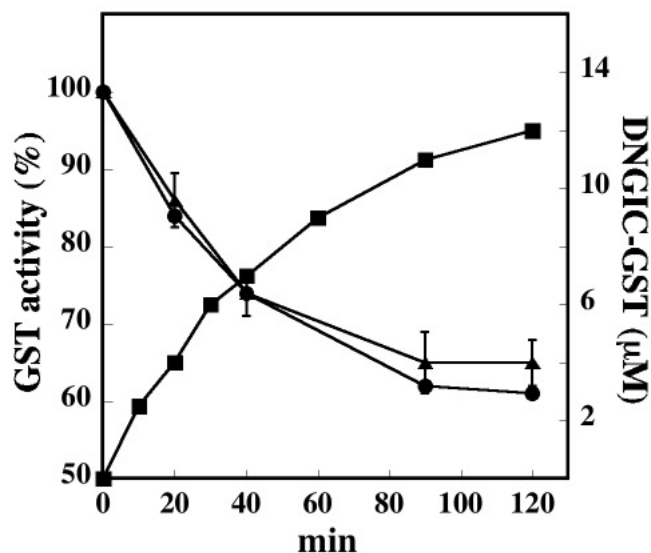


FIGURE 2.6. DNGIC-GST formation in intact hepatocytes. Rat hepatocytes (6×10^7 of cells in Krebs-Henseleit buffer) were incubated with 1 mM GSNO at 25°C. At variable times, aliquots of the cells were collected by centrifugation, sonicated, and centrifuged at $105,000 \times g$. The cytosolic fraction was then analyzed. ■, DNGIC-GST measured by EPR spectroscopy; ▲, GST activity; ●, theoretical inhibition for exclusive binding of DNDGIC to GSTs.

As in the homogenate, the EPR signal is stable for a few hours; this stability might be due to a steady-state equilibrium between decomposition and re-synthesis of the complex in the presence of an excess of GSNO. However, after repeated washing of the cells, the EPR signal is still stable for hours, thus suggesting that true stabilization occurs in the cell. At fixed times, hepatocytes were sonicated and centrifuged at $105,000 \times g$. The amount of cytosolic DNGIC-GST was measured by EPR spectroscopy and compared to the degree of GST inhibition. As found in the homogenate, the inhibition pattern parallels the DNDGIC formation and it also approaches the inhibition curve calculated for exclusive binding of DNDGIC to the endogenous GSTs (Fig. 2.6). Importantly, DNGIC-GST never exceeds the concentration of the intracellular GSTs pool; it actually approaches the concentration of the high affinity binding sites of GSTA1-1 (0.15 mM).

Interestingly, the $105,000 \times g$ pellet obtained from sonicated hepatocytes after GSNO treatment showed the presence of a bound DNIC with an EPR spectrum very similar to that of DNGIC-GST complex (Fig. 2.4). Further details were obtained by isolating nuclear, mitochondrial, lysosomal, and microsomal fractions after 1 hour of incubation of a rat liver homogenate with 1 mM GSNO. All subcellular fractions contain detectable amounts of the bound DNIC, but it is mainly localized in the nuclear fraction (Fig. 2.7).

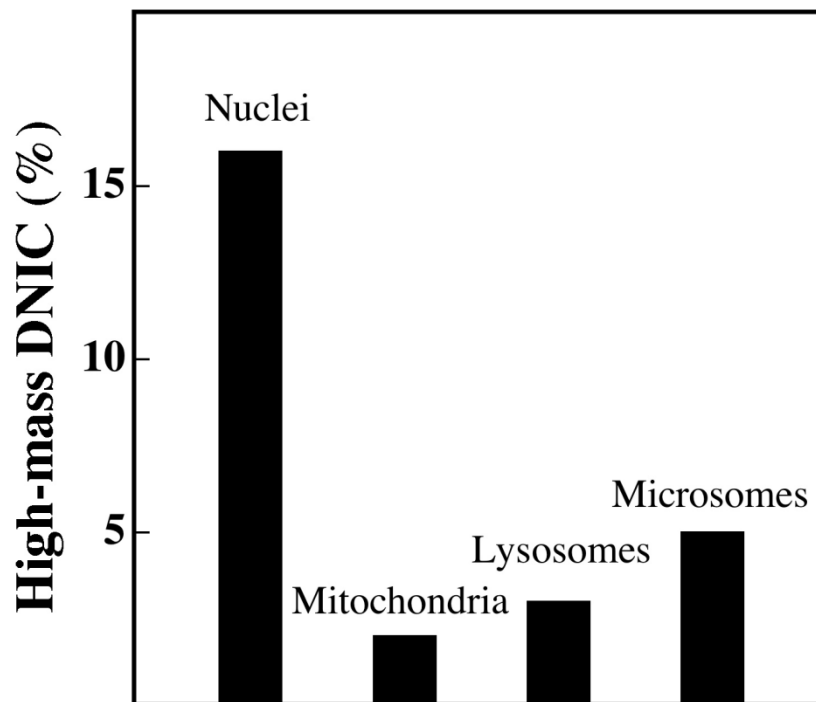


FIGURE 2.7. Subcellular association of high mass DNICs. Rat liver homogenate (18 μ M GSTs) was incubated with 1 mM GSNO for 60 min at 25°C. After incubation, nuclei, mitochondria, lysosomes, and microsomes were isolated by differential centrifugation, washed three times with 10 volumes of 0.25 M sucrose in 10 mM potassium phosphate buffer, pH 7.4, and analyzed by EPR spectroscopy. Values represent the percentage of DNIC compared with the total high mass DNIC found in the cytosol.

An identical distribution of bound DNICs was found by incubating separately each subcellular component with DNDGIC, indicating that the protein counterpart is constitutively bound to these fractions and not associated as a consequence of DNDGIC binding. As Alpha and Mu GSTs are considered cytosolic enzymes and

the peculiar membrane-bound microsomal MGST1 is found to have scarce affinity for DNDGIC, these results might indicate the presence of unknown proteins associated with subcellular organelles, able to bind DNDGIC but different from cytosolic GSTs.

2.3.4 Ferritin is the iron source for DNDGIC in hepatocytes

The level of GST-DNDGIC produced in intact hepatocytes after exposure to GSNO suggests a relevant mobilization of iron inside the cell. In hepatocytes, the cytosolic free iron pool is about 5 μM (22), a concentration two orders of magnitude lower than that of the DNDGIC formed in the cell after GSNO treatment. It has previously been reported that iron can be mobilized from ferritin by NO-generating systems (23). We confirm here that, in the presence of GSNO and GSH, iron is readily extracted from purified horse ferritin to produce free DNDGIC (Fig. 2.8a), similar results are obtained using transferrin as iron source. Interestingly, the kinetics of DNDGIC formation from ferritin and its final concentration are independent of the presence of GST (Fig. 2.8b and 2.8c), indicating that GST is not a kinetic or thermodynamic driving force for DNDGIC, but only binds the final complex.

While the kinetics of DNDGIC formation depends directly on GSNO concentration and on ferritin, the final amount of DNDGIC is determined by the amount of ferritin available (Fig. 2.8a). Importantly, only a small fraction of the iron present in the ferritin protein can be mobilized by GSNO (about 0.3%). The iron mobilization from horse ferritin also occurs in a complex milieu such as the crude homogenate. Addition of horse spleen ferritin to the rat liver homogenate in the presence of 1 mM GSNO and 10 mM GSH causes a net increase in the DNDGIC formed (Fig. 2.8d). This overproduction of DNDGIC corresponds to that calculated assuming that the homogenate does not alter the reaction observed with the purified system. Interestingly, the amount of iron extractable from the endogenous rat liver ferritin appears 10 fold higher than that coming from the purified horse spleen protein.

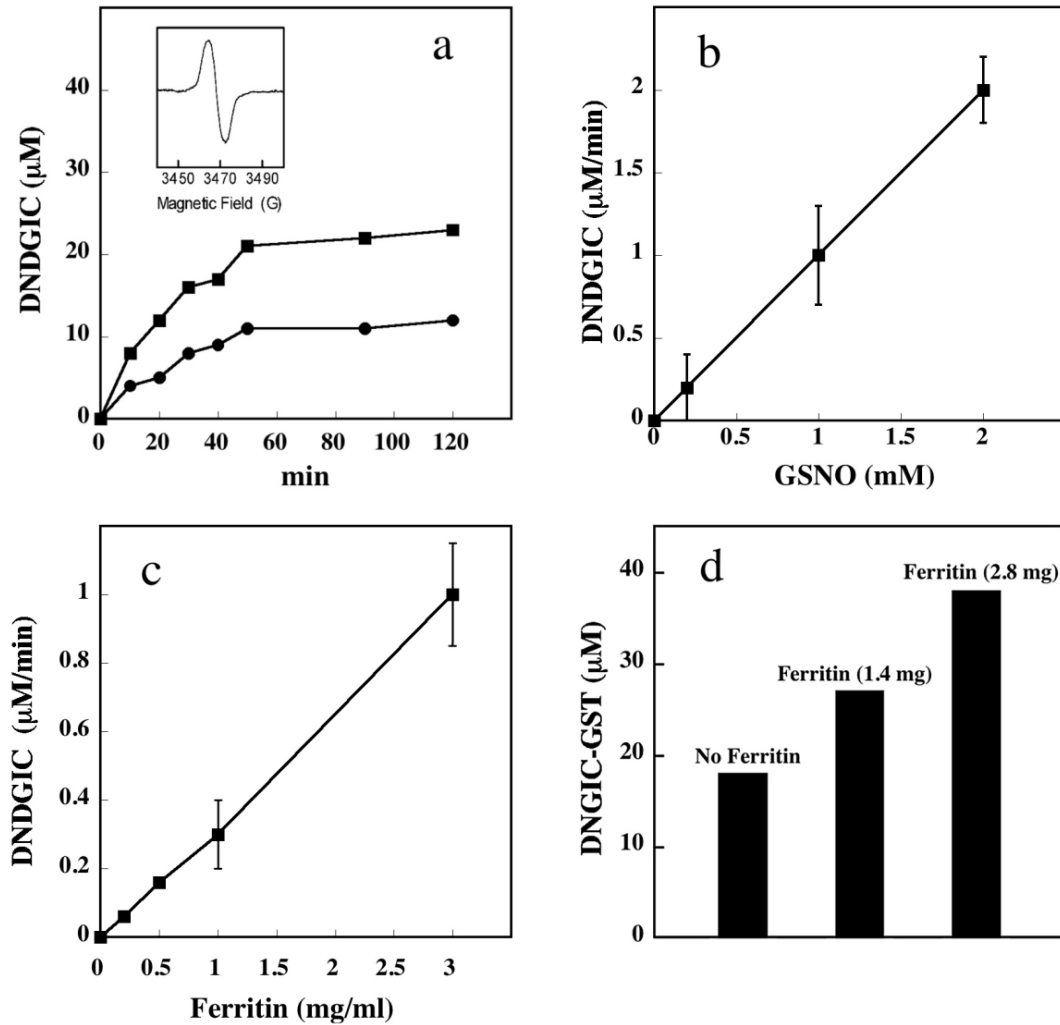


FIGURE 2.8. DNDGIC formation from horse ferritin, GSH, and GSNO. *a*, horse spleen ferritin was incubated in 1 ml of 10 mM GSH and 1 mM GSNO in 0.1 M potassium phosphate buffer, pH 7.4, at 25°C. At variable times, DNDGIC was measured by EPR measurements. ●, ferritin 1.4 mg/ml (final concentration) (estimated 4 mM total iron); ■, ferritin 2.8 mg/ml (final concentration) (estimated 8 mM total iron). The iron extracted by GSH and GSNO is about 0.3%. *b*, horse spleen ferritin (3 mg/ml) was incubated with variable amounts of GSNO and 10 mM GSH in 0.1 M potassium phosphate buffer, pH 7.4. At variable times the rate of DNDGIC was measured by EPR analysis or by the extent of GST inhibition, as described previously (10). *c*, variable amounts of horse spleen ferritin were incubated with 1 mM GSNO and 10 mM GSH in 0.1 M potassium phosphate buffer, pH 7.4. At variable times the rate of DNDGIC was measured by EPR analysis or by the extent of GST inhibition. *d*, rat liver homogenate was implemented with 1.4 or 2.8 mg/ml of horse spleen ferritin and incubated with 10 mM GSH and 1 mM GSNO in 0.1 M potassium phosphate buffer, pH 7.4. At various times the amount of DNDGIC was measured by EPR spectroscopy.

In fact, the total ferritin iron present in our homogenate is about 1 mM while the final concentration of DNDGIC is 28 μ M (3%). A higher propensity for the iron mobilization of the rat ferritin compared to that of the horse protein has been observed previously in case of iron extraction by superoxide ions (24).

2.3.5 Glutathione reductase is protected by GSTs against irreversible inhibition by DNDGIC

It was demonstrated that DNDGIC irreversibly inactivates glutathione reductase (GR). This reaction was studied in details by Boese *et al.* (7) and the X-ray crystal structure of the DNDGIC-inactivated enzyme has been solved by Karplus and coworkers (8). It has been clearly demonstrated *in vitro* that free DNDGIC at micromolar levels ($IC_{50} = 3-4 \mu$ M) oxidizes irreversibly the essential thiol group of Cys 63 to sulphinic acid (8). We therefore tested whether the complex bound to GST was still able to inactivate GR. Exposure of rat hepatocytes to 1 mM GSNO does not cause any detectable inhibition of GR even after 120 min incubation although the estimated cytosolic concentration of GST-DNIC reaches 0.15 mM.

To prove the involvement of GSTs in this protection and to evaluate the maximal defense capacity of the cell, we compare the effects of increasing amounts of DNDGIC added to rat liver homogenate. Inactivation of GR is observed only when the GST activity is almost reduced to zero, *i.e.* when the “buffer” capacity of GST is exhausted (Fig. 2.9a). In a different experiment, a fixed quantity of DNDGIC, overstoichiometric to the endogenous GST pool, was incubated in homogenate previously implemented with variable amounts of GSTA1-1. Also in this case, the activity of GR is unaffected as long as the fixed DNDGIC concentration remains understoichiometric to the total GST level (Fig. 2.9b). These results demonstrate that Alpha GST acts as a potent protection system and allow us to predict that DNDGIC in hepatocytes can accumulate up to a level of 0.6-0.7 mM without doing any significant damage to the cell.

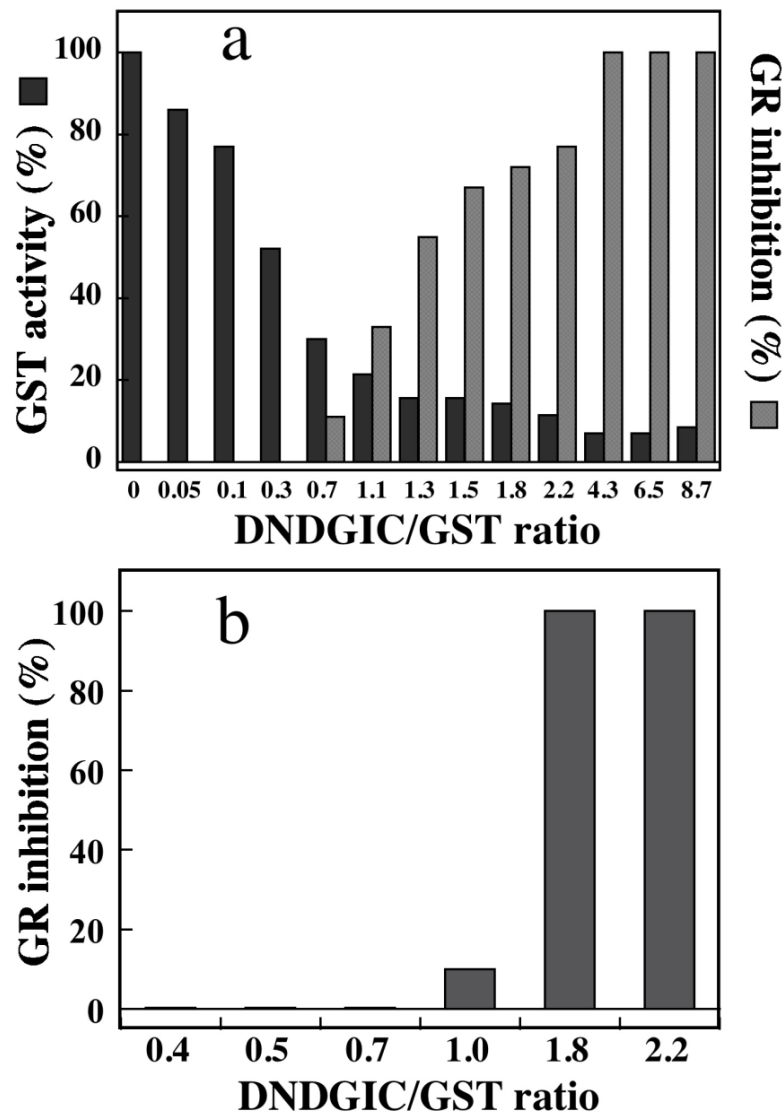


FIGURE 2.9. GSTs protect glutathione reductase against DNDGIC. *a*, rat liver homogenate (1:10 in 0.25 M sucrose) was incubated with variable amounts of DNDGIC (up to 8.7 molar excesses on endogenous GSTs) and 1 mM NADPH in 0.1 M potassium phosphate buffer, pH 7.4 (1 ml final volume). The final concentration of GSTs was 4.5 μ M. After 30 min, the activity of endogenous glutathione reductase was assayed as described under “Experimental Procedures.” No inhibition was observed even at the highest DNDGIC concentration in the absence of NADPH, as reported previously (7). *b*, rat liver homogenate (1:10 in 0.25 M sucrose) was incubated with a fixed DNDGIC concentration (10 μ M), 1 mM NADPH, and variable amounts of GSTA1-1 (up to 20 nmol/ml) in 0.1 M potassium phosphate buffer, pH 7.4 (1 ml final volume). After 30 min, the activity of endogenous glutathione reductase was assayed as described above.

2.4 Discussion

All these findings indicate the true occurrence *in vivo* of the interaction between the natural NO carrier DNDGIC and GSTs in intact hepatocytes. A first important finding is that this iron complex, when present at levels substoichiometric to GSTs, is almost exclusively sequestered by endogenous GSTs, even in a very complex protein milieu like a crude homogenate. In rat liver Alpha GSTs are the prime target of this interaction, whereas the Mu GSTs become effective only when the high affinity Alpha sites are saturated. This behavior could be predicted on the basis of the different dissociation constants for DNDGIC determined previously for each GST isoenzyme under purified conditions (11), but the present data demonstrate that the binding properties of these enzymes are unchanged in a complex protein milieu that approximates the *in vivo* conditions. Obviously, we cannot exclude that a small amount of DNDGIC bind to other proteins, but we can conclude that more than 95% of the complex is bound to GST in a 1:1 stoichiometric interaction.

In addition we show that DNDGIC is formed and successively stabilized by GSTs in a similar way both in a crude liver homogenate and in intact hepatocytes exposed to GSNO. The unique stoichiometric binding/inhibition pattern of the GST-complex interaction (observed both in intact hepatocytes and in a crude homogenate) reveals that the DNIC species formed in the cells is indeed the DNDGIC. This conclusion is important because the identity of intracellular DNIC species has never been established before. In hepatocytes DNDGIC is found entirely bound to GST and is never observed as the free complex. Preliminary data from our laboratory indicate that DNDGIC is formed and binds to GSTs also in other types of cells. Considering that GSTs are ubiquitous, and also Pi class GSTs bind the DNDGIC with high affinity, we propose that all the immobilized DNICs detected in biological systems through their characteristic EPR signal at $g = 2.03$ might be ascribed to intracellular DNGIC bound to GSTs.

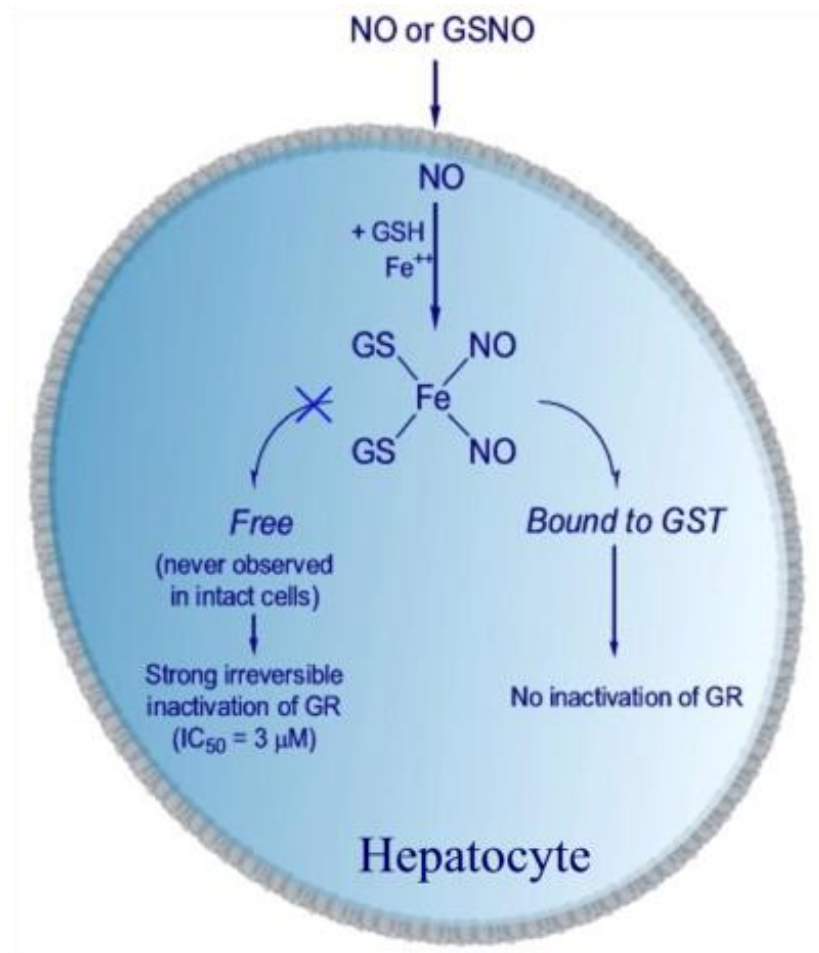
Because of the very high amounts of GSTs in hepatocytes, the final level of DNDGIC is always substoichiometric to the GSTs pool. Inhibition data confirm that Alpha GST is primarily involved in this interaction also in intact cells. Interestingly,

in the liver homogenate, a free form of DNIC produced by GSNO can be observed only when exogenous iron is added in amounts exceeding the GST concentration. Thus iron availability seems to be a crucial factor for DNIC accumulation in these multicomponent systems. In fact, experiments performed with purified horse ferritin indicate that this protein is the likely iron source for DNIC formation, but the iron released is only 0.3% of its total iron content. Although rat liver ferritin displays a 10-fold higher propensity to iron mobilization (about 3% of its iron content), the level of DNDGIC never exceeds the GST concentration. In any case, both iron extraction from ferritin or transferrin and the formation of DNDGIC depend only on the presence of NO together with high levels of GSH; no other cellular component is required for the reaction. This means that DNDGIC is generated spontaneously, and its accumulation in hepatocytes exposed to a flux of NO simply cannot be avoided. It appears likely that NO-mediated mobilization of iron from ferritin to form DNDGIC could somehow be related to GST expression, to ensure that practically all DNDGIC is bound to GSTs.

This may be critical for cell survival as DNDGIC is a potent inhibitor of glutathione reductase, causing the irreversible oxidation of Cys-63, a residue essential for catalysis. As proved here, this inactivation occurs only when DNDGIC is present as the free compound, *i.e.* when its concentration exceeds the binding capacity of the GST pool (0.6-0.8 mM). Thus GSTs, and in particular the Alpha class enzymes, represent a strong defense system in case of NO overloading or insult. Inhibition of GR is not the sole detriment coming from free DNDGIC.

The results described in this study may also explain the beneficial effect of NO against iron-mediated oxidative stress, observed previously in rat hepatocytes. Increased levels of labile iron (because of iron overload or to ethanol exposure) makes the cell more susceptible to oxidative stress. NO lowers the availability of the labile iron through DNDGIC formation (4). We can say now that this benefit is only possible because GSTs protect GR against the killer activity of DNDGIC, and at the same time because it avoids the extrusion of free DNDGIC that would cause iron depletion. Scheme 2.1 illustrates the basic principles of this protective mechanism. In this context it is interesting that preliminary results indicate that the sensitivity to NO of some parasites like *Plasmodium falciparum* could be related to

the prevalent expression of GST classes with no affinity or scarce affinity for DNDGIC in these organisms. Overall, these results depict a scenario for the cell in which cytotoxic effects of NO could be determined by the intracellular levels of GSTs and by their intrinsic affinity for DNDGIC.



SCHEME 2.1

2.5 References

1. Ueno, T., and Yoshimura, T. (2000) *Jpn. J. Pharmacol.* **82**, 95-101
2. Stadler, J., Bergonia, H. A., Di Silvio, M., Sweetland, M. A., Billiar, T. R., Simmons, R. L., and Lancaster, J. R. (1993) *Arch. Biochem. Biophys.* **302**, 4-11
3. Vanin, A. F., Blumenfeld, L. A., and Chetverikov, A. G. (1967) *Biophysics (Engl. Transl. Biofizka)* **12**, 829-841
4. Sergent, O., Griffon, B., Morel, I., Chevanne, M., Dubos, M.-P., Cillard, P., and Cillard, J. (1997) *Hepatology* **25**, 122-127
5. Pellat, C., Henry, Y., and Drapier, J. C. (1990) *Biochim. Biophys. Res. Commun.* **166**, 119 -125
6. Vanin, A. F., Serezhenkov, V. A., Mikoyan, V. D., and Genkin, M. V. (1998) *Nitric Oxide* **2**, 224-234
7. Boese, M., Keese, M. A., Becker, K., Büsse, R., and Mülsch, A. (1997) *J. Biol. Chem.* **272**, 21767-21773
8. Becker, K., Savvides, S. N., Keese, M., Schirmer, R. H., and Karplus, P. A. (1998) *Nat. Struct. Biol.* **5**, 267-271
9. Lo Bello, M., Nuccetelli, M., Caccuri, A. M., Stella, L., Parker, M. W., Rossjohn, J., McKinstry, W. J., Mozzi, A. F., Federici, G., Polizi, F., Pedersen, J. Z., and Ricci, G. (2001) *J. Biol. Chem.* **276**, 42138-42145
10. Turella, P., Pedersen, J. Z., Caccuri, A. M., De Maria, F., Mastroberardino, P., Lo Bello, M., Federici, G., and Ricci, G. (2003) *J. Biol. Chem.* **278**, 42294-42299
11. De Maria, F., Pedersen, J. Z., Caccuri, A. M., Antonini, G., Turella, P., Stella, L., Lo Bello, M., Federici, G., and Ricci, G. (2003) *J. Biol. Chem.* **278**, 42283-42293
12. Cesareo, E., Parker, L. J., Pedersen J. Z., Nuccetelli, M., Mazzetti, A. P., Pastore, A., Federici, G., Caccuri, A. M., Ricci, G., Julian J., Adams, J. J., Parker, M. W., and Lo Bello, M. (2005) *J. Biol. Chem.* **280**, 42172-42180
13. Board, P. G., and Pierce, K. (1987) *Biochem. J.* **248**, 937-941
14. Ross, V. L., and Board, P. G. (1993) *Biochem. J.* **294**, 373-380

15. Lo Bello, M., Battistoni, A., Mazzetti, A. P., Board, P. G., Muramatsu, M., Federici, G., and Ricci, G. (1995) *J. Biol. Chem.* **270**, 1249-1253
16. Incerpi, S., Spagnuolo, S., Terenzi, F., and Leoni, S. (1996) *Am. J. Physiol.* **270**, C841-C847
17. Pedersen, J. Z., and Cox, R. P. (1988) *J. Magn. Reson.* **77**, 369-371
18. Oppenheimer, J. H., and Schwartz, H. L. (1985) *J. Clin. Investig.* **75**, 147-154
19. Yeh, H.-I., Hsieh, C.-H., Wang, L.-Y., Tsai, S.-P., Hsu, H.-Y., and Tam, M. F. (1995) *Biochem. J.* **308**, 69-75
20. Rouimi, P., Debrauwer, L., and Tulliez, J. (1995) *Anal. Biochem.* **229**, 304-312
21. Adang, A. E. P., Brussee, J., van der Gen, A., and Mulder, G. (1990) *Biochem. J.* **269**, 47-54
22. Petrat, F., de Groot, H., and Rauen, U. (2001) *Biochem. J.* **356**, 61-69
23. Reif, D. W., and Simmons, R. D. (1990) *Arch. Biochem. Biophys.* **283**, 537-541
24. Harris, L. R., Cake, M. H., and Macey, D. J. (1994) *Biochem. J.* **301**, 385-389

3. STUDY OF GST LOCALIZATION IN RAT HEPATOCYTES

3.1 Introduction

Despite most of GSTs are present in the cytosolic fraction a specific isoenzyme (MGST1) has been found associated to microsomal membrane. This specific GST is a peculiar trimeric integral GST discovered and characterized many years ago (1). GSTA4-4, a specific isoenzyme able to detoxify hydroxyalkenals, displays a widespread mitochondrial, peroxisomal, and cytosolic localization, but the plasma membrane also binds detectable amounts of this enzyme (2). Furthermore, the tight association of Alpha and Mu class GSTs with the microsomal membrane fraction of rat liver was demonstrated by Morgenstern *et al.* (3), and about 2% of the cytosolic GSTA1-1 has been found in the microsomal membrane of sheep liver cells (4). Immunohistochemical evidence suggested the presence of nuclear Alpha and Pi class GSTs in different human tissues, but these studies did not quantify the specific isoenzymes involved (5, 6). Other investigations claimed either the presence or the absence of nuclear compartmentalization of GSTs. In particular, McCusker *et al.* (7) did not report any detectable nuclear GST activity, whereas Soboll *et al.* (8), using a nonaqueous technique of cell fractionation, found that both Alpha and Mu GSTs are present in the nucleus. Other studies reported a nuclear localization of GSTs (9-11), but the identification of the specific isoenzyme(s) involved in this association and their quantification are uncertain.

This study reveals for the first time that beside a significant amount of Alpha GSTs inside the nucleus, an equivalent amount is found in electrostatic association with the outer nuclear membrane. This particular modality of interaction has been detailed in cells and model systems using confocal microscopy, immunostaining experiments, and molecular modeling.

3.2 Experimental Procedures

Materials - GSH, 1-chloro-2,4-dinitrobenzene (CDNB) and NBD-Cl, were obtained from Sigma-Aldrich and polyclonal antibodies against Alpha and Mu GSTs were from Calbiochem. Fluorescein-conjugated goat anti-rabbit IgG was from Vector Laboratories, Burlingame, CA. human GSTA1-1, GSTM2-2, and GSTP1-1 were expressed in *Escherichia coli* and purified as described previously (12-14).

Synthesis of NBDHEX - 6-(7-nitro-2,1,3-benzoxadiazol-4-ylthio)hexanol (NBDHEX) was synthesized as reported by Ricci *et al.* (15).

GST activity - GST activity was assayed by the standard test that in 0.1 M potassium phosphate buffer, pH 6.5, in the presence of 1 mM GSH and 1 mM 1-chloro-2,4-dinitrobenzene at 25°C. An isotonic enzymatic test for GST was also performed using standard phosphate-buffered saline buffer, pH 6.5, containing 1 mM GSH and 1 mM CDNB. The reaction was followed spectrophotometrically at 340 nm where the GSH-2,4-dinitrobenzene adduct absorbs ($\epsilon = 9,600 \text{ M}^{-1} \text{ cm}^{-1}$). Activity of nuclear GST was measured by diluting aliquots of a nuclear suspension in the standard assay mixture or using the isotonic test described above. After 2min of preincubation, the time course of the reaction was linear. A similar procedure was used for activity determination in the mitochondria and microsome and lysosome fractions. With these activity measurements, it is not possible to distinguish whether the activity is because of GSTs inside the intact structures or due to GSTs bound to the outside of the membranes.

Cells - CCRF-CEM cells (human T-lymphoblastic leukemia) were grown as described previously (16). Hepatocytes were prepared from Wistar male rats as described in the accompanying paper (4). Experiments were carried out in accordance to the ethical guidelines for animal research (Communication of the Italian Ministry of Health).

Preparation of subcellular fractions - Subcellular fractions were prepared and characterized as reported (in the second part of this thesis) except that two parallel procedures were used; one procedure used a saline isotonic solution (0.05 M KCl, 0.04 M KH₂PO₄, and 0.1 M sucrose, pH 7.4), and the other procedure used a pure 0.25 M sucrose without salts.

Purification of weakly and tightly bound GSTs - The nuclear fraction obtained from 10 g of liver was washed three times with 20 ml of 0.25 M sucrose and resuspended in 20 ml of 0.25 M sucrose containing 10 mM potassium phosphate buffer, pH 7.4. The suspension was rapidly centrifuged at 1000 × g, and the procedure was repeated. Further rapid extractions did not increase the amount of GSTs in the supernatant. The collected supernatants were concentrated and represent the “weakly bound GSTs”. The pellet was again resuspended in the same buffer solution and incubated under gentle agitation for 1 h. This procedure was repeated three times. The collected supernatants were concentrated and represent the “tightly bound GSTs.” Both weakly and tightly bound GSTs were purified by affinity chromatography through a column (1 × 4 cm) of glutathione-Sepharose matrix (17). The first eluate was again passed through the column to retain quantitatively the Alpha GSTs.

SDS-PAGE and immunoblot analysis - Protein samples were analyzed by SDS-PAGE, visualized with Coomassie Brilliant Blue R-250, and transferred to Hybond-ECL nitrocellulose membranes (GE Healthcare). The proteins were immunoblotted with either a polyclonal anti-Alpha GST antibody or a polyclonal anti-Mu GST antibody.

HPLC analysis of GSTs - The GSTs extracted from nuclei were resolved on a reverse-phase (C18, 4.6 mm × 250 mm) column, essentially as reported by Yeh *et al.* (18).

Fluorescence labeling of GSTA1-1 and GSTM2-2 – 1 mM of NBD-Cl was reacted with 10 μ M purified human GSTA1-1 or GSTM2-2 in 0.1 M potassium phosphate buffer, pH 6.0. After 2 h the excess of reagent was removed by G-25 Sephadex chromatography, and the modified enzymes were analyzed spectrophotometrically. The selective alkylation of enzyme cysteines was confirmed on the basis of the diagnostic absorption peak centered at about 430-440 nm.

Immunofluorescence studies - The nuclei pellet was fixed in 4% freshly depolymerized paraformaldehyde in 0.25 M sucrose for 4 h at 4°C. After extensive washings in 0.25 M sucrose, floating pellets were incubated with a polyclonal anti-Alpha GST diluted 1:100 in 0.25 M sucrose overnight at 4°C and washed again in 0.25 M sucrose for 20 min. Pellets were then incubated with fluorescein-conjugated goat anti-rabbit IgG diluted 1:200 in 0.25 M sucrose, for 1 h at room temperature, washed in 0.25 M sucrose, and finally mounted on slides with Vectashield (Vector Laboratories). Slides were observed in a laser scanning confocal microscope (Nikon), and micrographs were digitally captured.

EPR spectroscopy - EPR measurements were made as described previously in part (2) of this thesis.

Confocal imaging - Confocal images were acquired with a confocal laser scanning microscope, Nikon PCM 2000 (Nikon Instruments) equipped with Spectra Physics Ar ion laser (488 nm, 514 nm) and He-Ne laser (543.5 nm) sources. A60 \times /1.4 oil immersion objective was used for the observations.

Electrostatic calculations - Molecular structures of human and rat GSTs were derived from the following Protein Data Bank entries: 2GSD (human A1-1), 2GTU (human M2-2), 6GSS (human P1-1), 1EV4 (rat A1-1), and 1B4P (rat M2-2). Protein charges were calculated by using the PDB2PQR software (19), and Poisson-Boltzmann calculations of electrostatic potential were performed with the APBS program (20), with 161 \times 161 \times 161 grid points, a 110-Å coarse grid and an 83-Å fine grid dimension, dielectric constants equal to 2 and 78.54 for protein and water,

respectively, and Debye-Hückel boundary conditions. Protein dipoles were estimated by employing the Dipole server, and molecular graphics were realized with the MOLMOL (21) and Chimera software (22).

3.3 Results

3.3.1 Detection of GSTs bound to subcellular components of rat hepatocytes

Many peripheral membrane proteins can easily be detached with mild treatments like increasing the ionic strength. Most standard procedures for the isolation of subcellular components include the use of buffered solutions thus some of the electrostatic protein-membrane interactions occurring in intact cells may be lost. In our study on the cellular compartmentalization of GSTs, we used only an isotonic solution of sucrose (0.25 M) for homogenization of the liver, as well as for isolation of the subcellular components. In addition, we adopted a particular GST activity determination on intact organelles (see “Experimental Procedures”) that avoids inactivation caused by sonication steps or by detergent extractions. As shown in Table 3.1, crude nuclear, lysosomal, mitochondrial, and microsomal fractions all contain GST activity.

Table 3.1. Subcellular localization of GST activity.

Activity measurements were done on intact organelles, isolated in pure sucrose (0.25 M) or in 0.1 M sucrose, 0.05 M KCl, and 0.04 M KH₂PO₄, pH 7.4, using the isotonic assay medium described under “Experimental Procedures.”

| Cell components | GST (units/g tissue) | |
|-----------------|----------------------|--------------------------------------|
| | Sucrose | Sucrose + potassium phosphate buffer |
| Cytosol | 101 ± 8 | 110 ± 10 |
| Nuclei | 16 ± 2 | 8 ± 2 |
| Mitochondria | 1.6 ± 0.4 | 0.7 ± 0.3 |
| Lysosomes | 2.9 ± 0.7 | 1.6 ± 0.2 |
| Microsomes | 4.2 ± 1 | 2.1 ± 0.4 |

The highest activity was recovered in the nuclear pellet that contained an amount corresponding to about 15% of the overall cytosolic GST activity. Interestingly, about 50% of the GST activity of the fractions is lost when the subcellular components are isolated in isotonic saline solution (Table 3.1), suggesting that about half of the GST could be electrostatically bound. Because of the considerable amount of GST activity associated with the nuclear pellet, only this specific subcellular fraction was further studied and characterized.

3.3.2 Nuclear pellet of hepatocytes displays GST activity

The nuclear pellet from rat liver, isolated after homogenization in 0.25 M sucrose (1:10), was washed three times with 10 volumes of sucrose 0.25 M to remove any contamination of the cytosolic GSTs. Optical microscopy showed that the nuclei were intact. The nuclear pellet resuspended in 0.25 M sucrose contained a total of 16 GST units per g of tissue. After treatment of nuclei with 10 volumes of 10 mM potassium phosphate buffer or 20 mM NaCl in the presence of 0.25 M sucrose, about 8 units were released into the surrounding solution, confirming the presence of GSTs electrostatically bound to the nuclei (weakly bound GST). No additional release was observed after increasing the concentration of the buffer up to 0.1 M. The remaining activity associated with the nuclear pellet, termed tightly bound GST (about 8 units), could only be partially extracted by multiple and prolonged incubations (1 h each) with 10 volumes of 0.25 M sucrose in 10 mM potassium phosphate buffer. Sonication treatment of the nuclear pellet or the use of detergents like Triton X-100 even at low concentrations (1%) caused partial and irreversible inactivation of the enzyme. The use of concentrated carbonate did not increase the rate and extent of the extraction, indicating that the tightly bound GST did not behave like a peripheral protein (4). The most likely localization of the tightly bound GST is the nuclear interior, as indicated by confocal microscopy (see below).

Further evidence of the presence of equivalent levels of GSTs associated with the nucleus was provided by EPR spectroscopy. It has been demonstrated that the paramagnetic species DNDGIC binds tightly to Alpha and Mu GST with 1:1 stoichiometry, giving an EPR spectrum different from that of the free complex (23). Titration of GSTs with DNDGIC therefore allows quantification of GSTs. Experiments performed on nuclei isolated in 0.25 M sucrose or in saline solution are shown in Fig. 3.1 where the loss of activity because of the binding of DNDGIC is also reported. Starting from a rat liver of 10 g (51 mg of total GSTs), the weakly bound GST was about 5mg and a similar amount was recovered as tightly bound GST.

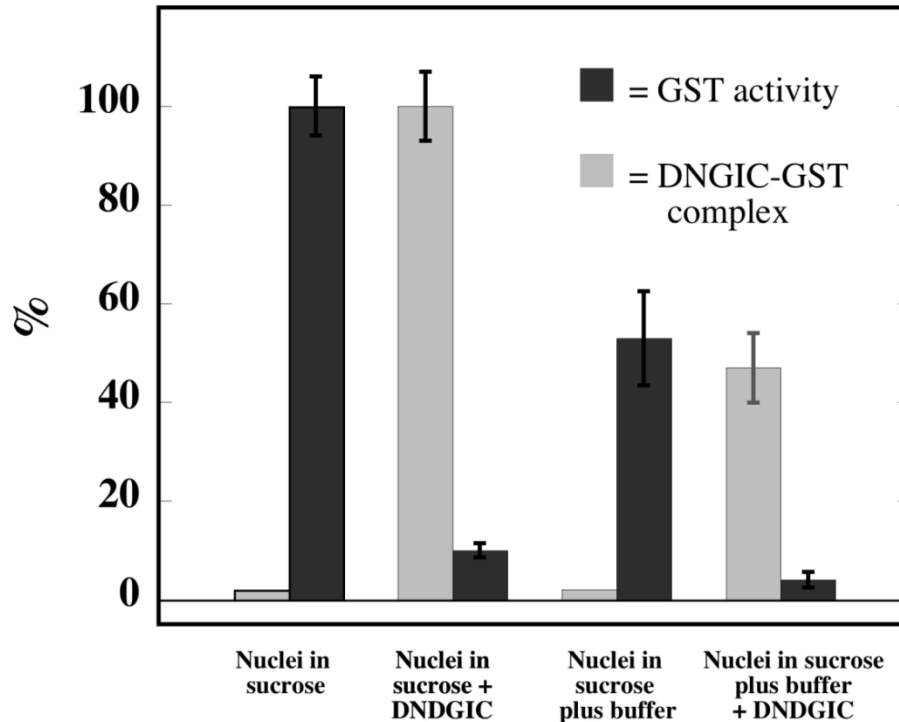


FIGURE 3.1. Titration of the nuclear GST with DNDGIC. The nuclear pellet isolated in 0.25 M sucrose is incubated with 10 volumes of 10 μ M DNDGIC at pH 7.4. After removal of the free complex by G-25 Sephadex chromatography, GST activity under isotonic conditions and EPR quantifications are performed as described under “Experimental Procedures.” The same experiment is performed with the nuclear pellet isolated in 10 mM potassium phosphate buffer, pH 7.4, and 0.25 M sucrose. Data are the means \pm S.D. of three experiments.

3.3.3 GSTA1-1 and GSTA2-2 are associated to the nuclear membrane

The extracts containing the solubilized weakly and tightly bound GSTs contain other proteins as well. In fact, they display specific activities of \sim 3 units/mg that rise to 16 units/mg after glutathione-Sepharose affinity chromatography. SDS-PAGE, performed after the affinity step, indicates that these samples have similar protein composition (Fig. 3.2a) with a main component at about 25 kDa and a minor component of 24 kDa (about 20%). The immunoblot in Fig. 3.2b shows that only the major component at 25 kDa cross-reacts with the anti-Alpha GST antibody, whereas neither the 25 kDa nor the 24 kDa component react with the anti-Mu GST antibody.

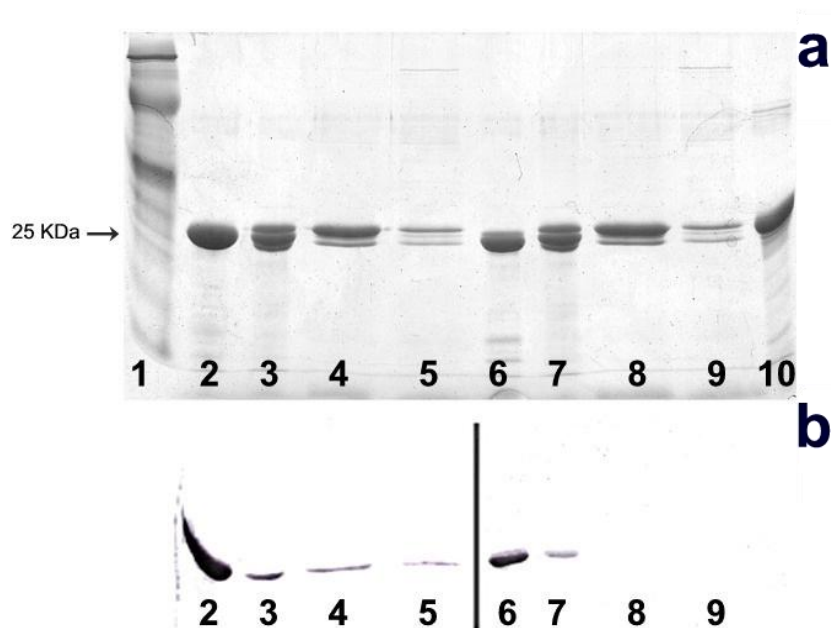


FIGURE 3.2. SDS-PAGE and immunoblotting. *a*, SDS-PAGE. *Lane 1*, protein markers; *lane 2*, purified human GSTA1-1; *lanes 3 and 7*, purified pool of cytosolic GSTs isoenzymes; *lanes 4 and 8*, weakly bound GST; *lanes 5 and 9*, tightly bound GST; *lane 6*, purified human GSTM2-2; *lane 10*, GSTP1-1 used as negative control. *b*, immunoblotting using anti-Alpha GST (*left side*) and anti-Mu GST (*right side*).

The minor component, which neither belongs to the Alpha nor to the Mu class, has not yet been further analyzed. To identify the specific Alpha isoenzyme(s) involved in the weak and tight association, a simple reversed phase HPLC analysis was performed, according to the procedure described by Yeh *et al.* (18). The weakly bound GSTs are mainly represented by GSTA1-1, GSTA2-2, and GSTA3-3, approximately with the same relative abundance as found in the cytosol. Conversely, the tightly bound GSTs are mainly represented by GSTA1-1 and GSTA3-3 (Fig. 3.3).

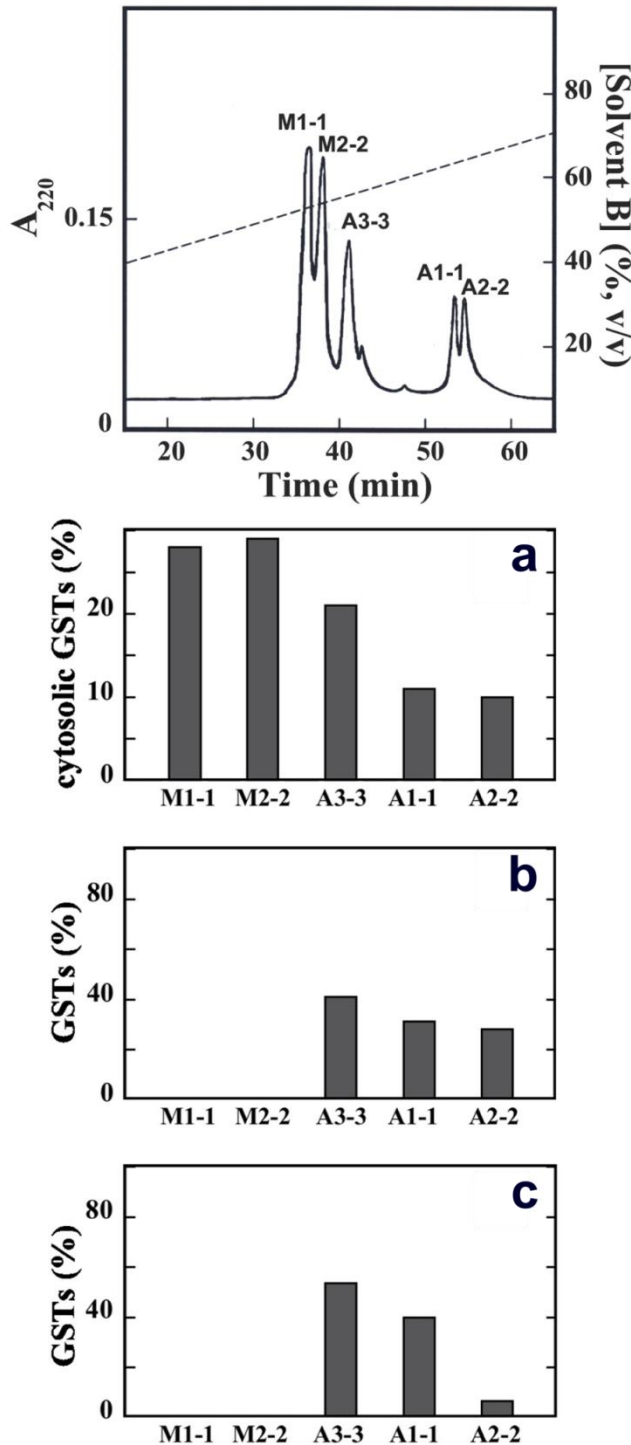


FIGURE 3.3. HPLC analysis. Tightly and weakly bound GSTs, extracted as reported under “Experimental Procedures”, were purified through affinity chromatography and analyzed by reverse phase HPLC as described previously (18). Identification of GST isoenzymes were made according to Ref.18. *Upper panel*, representative chromatogram of the cytosolic GSTs, previously purified through two subsequent affinity chromatography steps on glutathione- Sepharose matrix (17) (recovery $\geq 93\%$). *a*, relative amounts of the five cytosolic isoenzymes present in the GST pool. Isoenzymes below 2% are not reported. The total amount of cytosolic GSTs is 5.1 mg/g liver. *b*, relative amounts of isoenzymes of the weakly bound GSTs. The total amount of the weakly bound GSTs is 0.5 mg/g liver, corresponding to 10% of the cytosolic GSTs. *c*, relative amounts of isoenzymes of the tightly bound GSTs. The amount of the tightly bound GSTs after partial extraction (60%) is 0.3 mg/g liver, corresponding to 6% of the cytosolic GSTs. The nomenclature used for rat GST isoenzymes is in accordance with the one proposed recently (24). Percentages represent the mean of three experiments.

3.3.4 Evidence of the association of Alpha GSTs to the nuclear membrane

Direct evidence of intranuclear and perinuclear association of Alpha GSTs is provided by confocal fluorescence microscopy using an anti-Alpha GST antibody and a secondary fluorescent antibody. All nuclei display intense staining at the periphery but also inside the nuclei (Fig. 3.4).

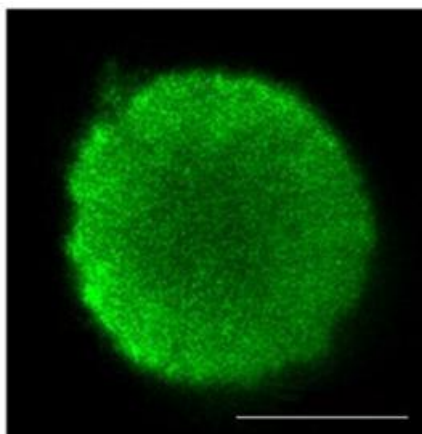


FIGURE 3.4. Immunofluorescence.

High power oil-immersion confocal micrograph of nuclei pellets immunoreacted with anti-Alpha GST, diluted 1:100, followed by fluorescein-conjugated secondary antibody (see “Experimental Procedures”). Bar, 5 μm .

NBDHEX, a specific fluorescent probe for Alpha GST, gives further confirmation. It has been demonstrated recently that this fluorescent compound, able to trigger apoptosis in human tumor cells, acts as a strong inhibitor of Alpha, Pi, and Mu GSTs by binding tightly to the active site of these enzymes (15). Interaction of this compound with Mu and Pi GSTs causes a dramatic loss of its intrinsic fluorescence, whereas the fluorescence spectrum is almost unchanged when NBDHEX binds to Alpha GST ($K_D = 5.3 \times 10^{-6}$ M) (15). Incubation of intact nuclei with 10 μM NBDHEX causes a distinct accumulation of fluorescence at the nuclear membrane and also faint fluorescence inside the nucleus (Fig. 3.5). When the same experiment was performed with nuclei extensively washed with 10 mM potassium phosphate buffer, only faint intranuclear fluorescence was observed (not shown).

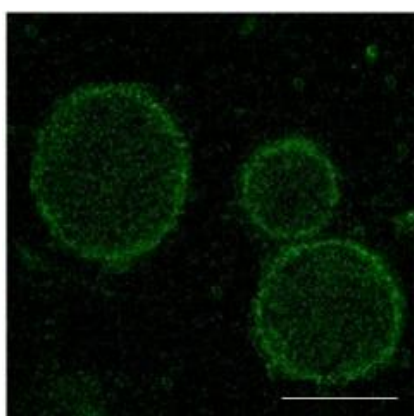


FIGURE 3.5. Fluorescence label experiments. Nuclei pellets incubated with NBDHEX. Bar, 10 μm .

3.3.5 Binding of Alpha GST to the nuclear membrane is not an artifact?

The data reported above prove that a part of the intracellular GST pool is associated with the nucleus. However, they do not exclude the possibility that this association might not be present in the intact hepatocyte but is induced artificially by the homogenization in sucrose in the absence of buffer or other inorganic salts. Convincing evidence that this interaction really occurs in intact cells is achieved using NBDHEX as a fluorescent intracellular marker for Alpha GSTs. NBDHEX not only specifically labels GSTs but also accumulates in the cell within a few minutes (25). After exposure of rat hepatocytes to 0.1 mM NBDHEX, faint fluorescence is visible in the cytosol, but also a strong staining of the nuclei, mainly localized on the nuclear envelope (Fig. 3.6).

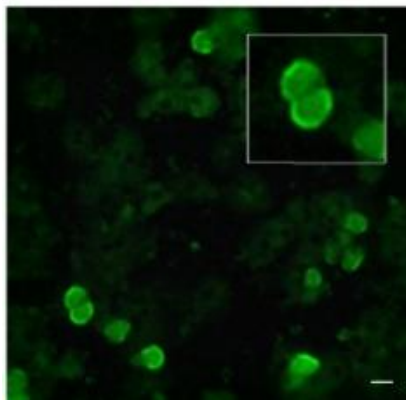


FIGURE 3.6. Fluorescence label experiments of hepatocytes. Intact rat hepatocytes incubated with NBDHEX. Bar, 12 μm . The inset shows a 2-fold magnification.

To verify if NBDHEX labels selectively GSTs and to prove the absence of nonspecific interactions with the nuclear membrane, rat hepatocytes were incubated with 1 mM GSNO after treatment with NBDHEX. As DNDGIC binds to Alpha GSTs with an affinity a thousand times higher than NBDHEX ($K_D = 10^{-10}$ M), the iron complex will displace this fluorescent label. The fluorescence observed after exposure to NBDHEX and localized near the nuclear envelope fades almost completely after 1 h of incubation with 1 mM GSNO (Fig. 3.7).

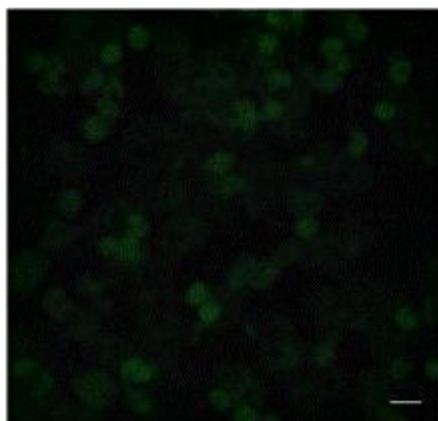


FIGURE 3.7. Fluorescence label experiments of hepatocytes. Rat hepatocytes, treated with NBDHEX and exposed to 1 mM GSNO for 1 h. Bar, 20 μ m.

The absence of nonspecific binding of NBDHEX to the membrane was also demonstrated by exposing a human tumor cell line (CEM) to NBDHEX. These tumor cells do not express Alpha or Mu GSTs but exclusively the Pi class GSTP1-1. After incubation with 50 μ M NBDHEX, the nuclei appear like black holes, whereas a detectable fluorescence is visible in the cytosol, indicating that NBDHEX enters the cells (Fig. 3.8).

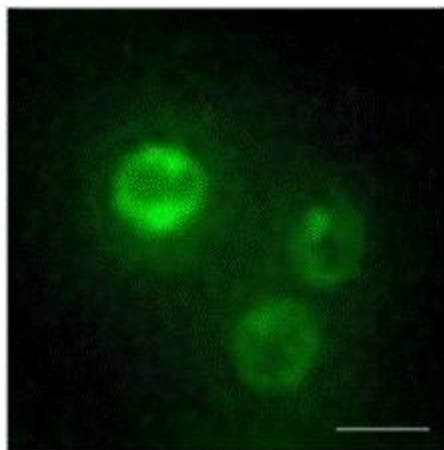


FIGURE 3.8. Fluorescence label experiments of CEM. Low power confocal micrograph of CEM cells incubated with NBDHEX. Bar, 20 μ m.

3.3.6 Molecular modeling of GST electrostatics

A more detailed analysis of the electrostatic properties of the GST isoenzymes provides further information regarding the mode of association. In addition to a net positive charge, GSTA1-1 also exhibits an asymmetric distribution of electric

charges, which endows this protein with a strong electric dipole (1000 Debye, as calculated by the Dipole server), as shown in Fig. 3.9. Interestingly, this was not the case for the other isoenzymes (the calculated electric dipoles of GSTM2-2 and P1-1 are 240 and 40 Debye, respectively). A further illustration of this point is provided by a calculation of the electrostatic potential generated by GSTs, performed by solving the Poisson-Boltzmann equation with the APBS software (20).

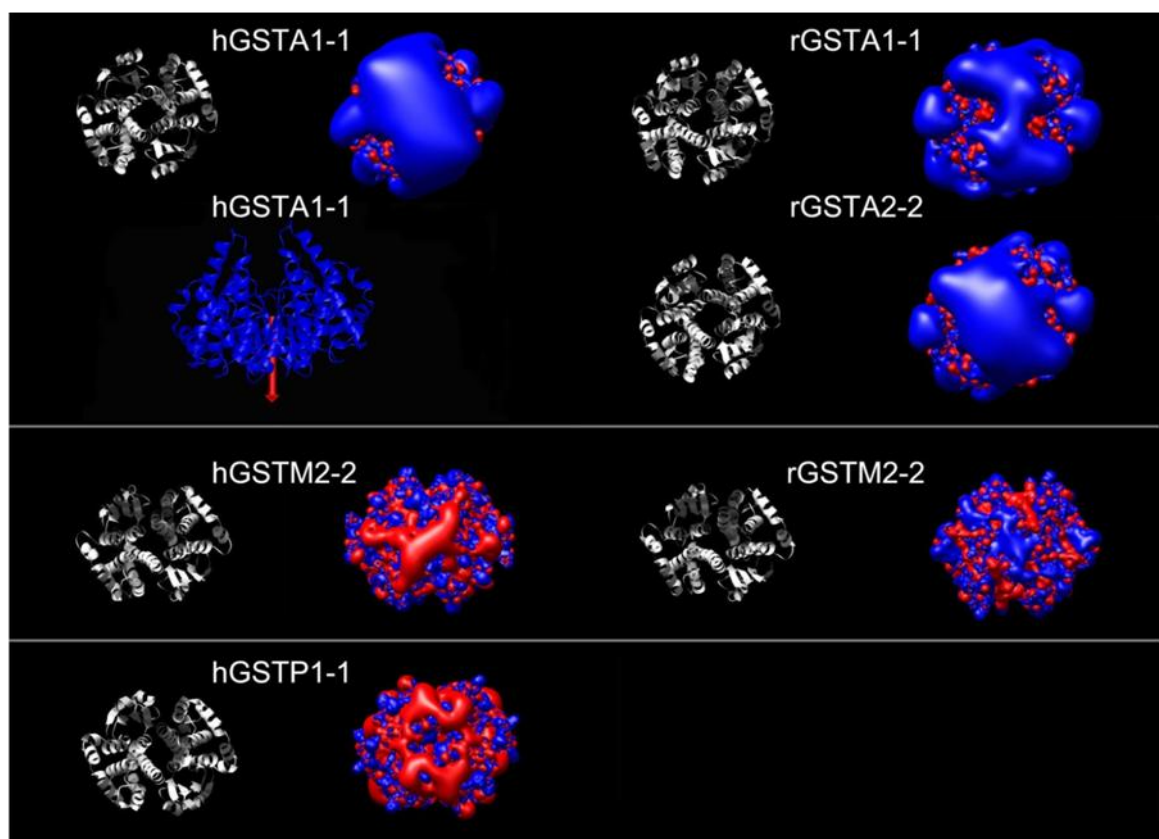


FIGURE 3.9. Electrostatic calculations. Models represent the crystal structures of GSTA1-1, GSTM2-2, and GSTP1-1 and their isotopotential surfaces corresponding to -3 kT/e (in blue) and $+3$ kT/e (in red). Only GSTA1-1 shows a significant positive potential on the surface of the dimer located on the protein side opposite to the active sites. In the model of *hGSTA1-1*, a dipolar moment of 1000 Debye was calculated and is represented as a red arrow inside the dimer.

Fig. 3.9 shows the isotopotential surfaces corresponding to $+3$ kT/e (in blue) and -3 kT/e (in red), demonstrating a significant positive potential on the surface of the dimer located on the protein side opposite to the active sites. Very likely this is the protein region interacting electrostatically with the membrane. In agreement with

this conclusion, a positive potential region was not present in the other isoenzymes, which did not interact with the nuclear membrane or with liposomes. It is worth noting that very similar results were obtained for both human and rat enzymes (data not shown).

3.3.7 Quantitation of GSTs bound electrostatically

Quantitation of the GSTs involved in subcellular compartmentalization in rat hepatocytes indicates that about 20% of cytosolic Alpha class GSTs are electrostatically associated with the outer nuclear membrane, and an equivalent amount is present in the nuclear interior. The level of the cytosolic Alpha GSTs is about 2.2 mg/g of liver (reaching a concentration of 0.3 mM in the cytosol, 43% of the total GSTs), whereas about 0.5 mg is electrostatically associated with the nuclear membrane, and an equivalent amount is probably compartmentalized inside the nucleus. As the nuclear volume is about 10% of the cytosolic volume, the intranuclear GST concentration may be 0.7 mM, a value comparable with that found in cytosol. This concentration may reflect a free diffusional in/out traffic of Alpha GSTs between the cytosolic and nuclear compartments.

Notably, the nuclear access seems to be denied for Mu GSTs. In contrast, the local concentration of Alpha GSTs at the outer nuclear membrane will be much higher. An estimation of the minimum surface occupied by all electrostatically bound GSTA1-1 assembled in a layer (calculated on the basis of an area of 19.6 nm² for each GSTA1-1 dimer, based on the X-ray structure) paradoxically results about five times larger than the surface of the entire nuclear membrane (Table 3.2). In addition, the specific activity of the Alpha GSTs, extracted from the nuclear membrane after salt treatment, is about 3 units/mg, five times lower than that of the purified enzymes (16 units/mg). Thus, other proteins must be electrostatically associated with the nuclear envelope together with GSTs; this appears to be an additional paradox, given the absence of free membrane area for further electrostatic interactions. One possible explanation for this excessive amount of bound proteins is that Alpha GSTs could be assembled in a multilayer disposition near the nuclear membrane in an alternate sequence with negatively charged proteins.

Table 3.2. Quantitative analysis of GSTs bound electrostatically to subcellular membranes.

| Cell components | Membrane area ^a | GST/membrane area | Area of GSH/membrane area |
|-----------------|----------------------------------|--------------------------|---------------------------|
| | <i>m</i> ² / <i>g</i> | <i>mg/m</i> ² | |
| Nuclei | 0.022 | 22.7 | 5.0 |
| Mitochondria | 0.77 | 0.06 | 0.01 |
| Lysosomes | 0.044 | 2.4 | 0.5 |
| Microsomes | 5.5 | 0.02 | 0.01 |

^aData were derived from Ref. (26).

3.4 Discussion

Data reported above indicate that a few GST isoenzymes are involved in subcellular compartmentalization in rat hepatocytes. About 20% of cytosolic Alpha class GSTs are electrostatically associated with the outer nuclear membrane, and an equivalent amount is present in the nuclear interior. The use of 0.25 M sucrose without exogenous salts for nuclei isolation, and the particular assay for GST activity of intact nuclei, made it possible to discover this double modality of association that, to a lesser extent, may also be present in other subcellular components (see Table 3.1). Previous observations contrary to the nuclear compartmentalization of GST were probably because of the use of standard subcellular fractionation procedures that caused the loss of the electrostatically bound GST, and to the extensive inactivation that occurs during sonication of nuclei or extraction with detergents.

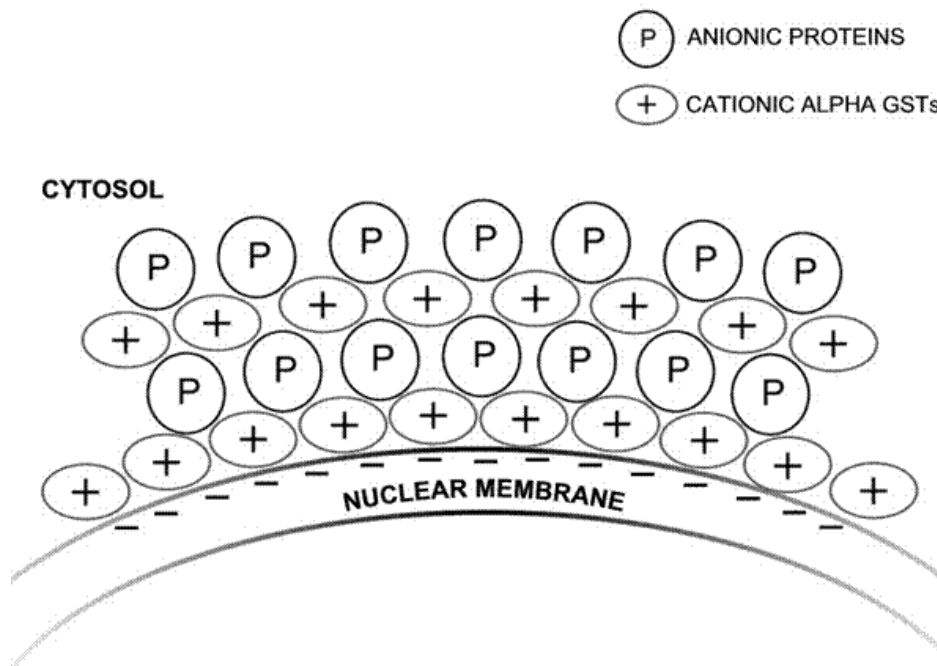
Immunostaining and chromatographic data indicate that GSTA1-1, GSTA2-2 and GSTA3-3 are the enzymes mainly involved in the nuclear association. Confocal microscopy and the use of NBDHEX, a specific fluorescent probe for Alpha GSTs, give a direct visualization of the presence of these isoenzymes both at the outer nuclear membrane and in the nuclear interior. The electrostatic binding of Alpha GSTs observed in isolated nuclei is well reproduced with liposomes, and the results also confirm that Mu and Pi class GSTs do not interact at physiological pH values. Finally, electrostatic potential calculations, performed on Alpha, Mu, and Pi GSTs indicate that only Alpha GSTs display a proper electrostatic potential at the protein surface to interact with the negatively charged membrane. In this context, another peculiar feature of the Alpha dimer is the strong dipolar character that is not found in the other GST isoenzymes.

An examination of the present data discloses a surprising scenario. The amount of the cytosolic Alpha GSTs is about 2.2 mg/g of liver (reaching a concentration of 0.3 mM in the cytosol, 43% of the total GSTs), whereas about 0.5 mg is electrostatically associated with the nuclear membrane, and an equivalent amount is probably compartmentalized inside the nucleus. As the nuclear volume is about 10% of the cytosolic volume, the results are that the intranuclear GST concentration

is ~ 0.7 mM, a value comparable with that found in cytosol. This concentration may reflect a free diffusional in/out traffic of Alpha GSTs between the cytosolic and nuclear compartments. Notably, the nuclear access seems to be denied for Mu GSTs. In contrast, the local concentration of Alpha GSTs at the outer nuclear membrane will be much higher. An estimation of the minimum surface occupied by all electrostatically bound GSTA1-1 assembled in a layer (calculated on the basis of an area of 19.6 nm² for each GSTA1-1 dimer, based on the X-ray structure) paradoxically results about five times larger than the surface of the entire nuclear membrane (Table 3.2). In addition, the specific activity of the Alpha GSTs, extracted from the nuclear membrane after salt treatment, is about 3 units/mg, five times lower than that of the purified enzymes (16 units/mg). Thus, other proteins must be electrostatically associated with the nuclear envelope together with GSTs; this appears to be an additional paradox, given the absence of free membrane area for further electrostatic interactions. One possible explanation for this excessive amount of bound proteins is that Alpha GSTs could be assembled in a multilayer disposition near the nuclear membrane in an alternate sequence with negatively charged proteins (Scheme 3.1). This peculiar onion layer-like assembly of proteins is not a complete novelty. It has been demonstrated *in vitro* that positively charged proteins easily aggregate in such a way to negatively charged colloidal particles in the presence of anionic polyelectrolytes (27, 28), and our preliminary results also indicate a prevalent anionic nature.

To our knowledge, the present data represent the first indication for the existence *in vivo* of a similar protein assembly, which obviously needs further confirmation. The possibility that a few cytosolic enzymes are not in a completely disordered distribution but electrostatically ordered near specific intracellular membranes opens a new and fascinating scenario in cell physiology. Is it possible that this hypothetical protein shell escaped visualization by advanced spectroscopy and microscopy techniques? The answer may be affirmative. We must remember that the protein concentration in the cytosol is above 300 mg/ml, a borderline value for protein crystallization. Thus all cytosolic proteins are extremely crowded, but no spectroscopic or microscopic evidence has been reported for this almost crystal-like

condition. Obviously in the absence of a detectable selective marker no trace can be expected if this crowding is formed by selected proteins near specific subcellular components. Whatever the true assembly of Alpha GSTs at the nuclear envelope, the presence of large amounts of these specific GSTs near the nucleus demonstrated here is a novelty and probably has a physiological finality. In fact, all GSTs represent a very efficient defense system against many toxic alkylating compounds, but Alpha class GSTs display an additional and peculiar peroxidase activity, not shown by Mu and Pi GSTs, and eliminate efficiently dangerous organic peroxides (29).



SCHEME 3.1

Alpha class GSTs also have a 10 times higher affinity than Pi and Mu GSTs for DNDGIC, a natural carrier of NO that displays strong oxidizing properties and inactivates irreversibly key enzymes like glutathione reductase (30, 31). Thus, the present results seem to indicate that the nucleus and its precious genetic content have a further mechanism of protection, not considered until now. Quite a few questions remain. For example, given the similar lipid composition of most intracellular membranes, it is not clear why the Alpha GST displays such an impressive accumulation on the nuclear membrane (see Table 3.2). Interestingly, it was shown many years ago by Virtanen (32) that the outside of the nucleus is strongly negatively charged, but the inner membrane is practically neutral. However, it is also possible that specific nuclear membrane proteins recognize Alpha GSTs and favor their accumulation. We did not explore in this study the status of the tightly bound GSTs that probably reside in the nuclear interior. The curiously similar amount of the “external” and “internal” Alpha GSTs could be merely a coincidence, or it could reflect a specular modality of interaction of Alpha GSTs with the outer and inner membrane. Work is in progress to answer these questions.

2.5 References

1. Morgenstern, R., DePierre, J. W., and Jornvall, H. (1985) *J. Biol. Chem.* **260**, 13976-13983
2. Singh, S. P., Janecki, A. J., Srivastava, S. K., Awasthi, S., Awasthi, Y. C., Xia, S. J., and Zimniak, P. (2002) *J. Biol. Chem.* **277**, 4232-4239
3. Morgenstern, R., Guthenberg, C., Mannervik, B., and DePierre, J. W. (1983) *FEBS Lett.* **160**, 264-268
4. Sandeep, K., Prabou, K. S., Reddy, P. V., Gumpricht, E., Hildenbrandt, G. R., Scholz, R. W., Sordillo, L. M., and Reddy, C. C. (2001) *Biochem. J.* **360**, 345-354
5. Campbell, J. A. H., Corrigan, A. V., Guy, A., and Kirsch, R. E. (1991) *Cancer* **67**, 1608-1613
6. Abei, M., Harada, S., Tanaka, N., McNeil, M., and Osuga, T. (1989) *Biochim. Biophys. Acta* **995**, 279 -284
7. McCusker, F. M., Phillips, M. F., Boyce, S. J., and Mantle, T. J. (1990) in *Glutathione S-Transferases and Drug Resistance* (Hayes, J. D., Pickett, C. B., and Mantle, T. J., eds) Taylor & Francis Ltd., London
8. Soboll, S., Grundel, S., Harris, J., Kolb-Bachofen, V., Ketterer, B., and Sies, H. (1995) *Biochem. J.* **311**, 889-894
9. Rogers, L. K., Gupta, S., Welty, S. E., Hansen, T. N., and Smith, C. V. (2002) *Toxicol. Sci.* **69**, 279-285
10. Bennett, C. F., Spector, D. L., and Yeoman, L. C. (1986) *J. Cell Biol.* **102**, 600-609
11. Rozell, B., Hansson, H. A., Guthenberg, C., Tahir, M. K., and Mannervik, B. (1993) *Xenobiotica* **23**, 835-849
12. Lo Bello, M., Nuccetelli, M., Caccuri, A. M., Stella, L., Parker, M. W., Rossjohn, J., McKinstry, W. J., Mozzi, A. F., Federici, G., Polizio, F., Pedersen, J. Z., and Ricci, G. (2001) *J. Biol. Chem.* **276**, 42138-42145
13. Board, P. G., and Pierce, K. (1987) *Biochem. J.* **248**, 937-941
14. Ross, V. L., and Board, P. G. (1993) *Biochem. J.* **294**, 373-380

15. Ricci, G., De Maria, F., Antonini, G., Turella, P., Bullo, A., Stella, L., Filomeni, G., Federici, G., and Caccuri, A. M. (2005) *J. Biol. Chem.* **280**, 26397-26405
16. Turella, P., Cerella, C., Filomeni, G., Bullo, A., De Maria, F., Ghibelli, L., Ciriolo, M. R., Cianfriglia, M., Mattei, M., Federici, G., Ricci, G., and Caccuri, A. M. (2005) *Cancer Res.* **65**, 3751-3761
17. Simmons, P. C., and Vander Jagt, D. L. (1977) *Anal. Biochem.* **82**, 334-341
18. Yeh, H.-I., Hsieh, C.-H., Wang, L.-Y., Tsai, S.-P., Hsu, H.-Y., and Tam, M. F. (1995) *Biochem. J.* **308**, 69-75
19. Dolinsky, T. J., Nielsen, J. E., McCammon, J. A., and Baker, N. A. (2004) *Nucleic Acids Res.* **32**, W665-W667
20. Baker, N. A., Sept, D., Joseph, S., Holst, M. J., and McCammon, J. A. (2001) *Proc. Natl. Acad. Sci. U. S. A.* **98**, 10037-10041
21. Koradi, R., Billeter, M., and Wüthrich, K. (1996) *J. Mol. Graphics* **14**, 51-55
22. Pettersen, E. F., Goddard, T. D., Huang, C. C., Couch, G. S., Greenblatt, D. M., Meng, E. C., and Ferrin, T. E. (2004) *J. Comput. Chem.* **25**, 1605-1612
23. De Maria, F., Pedersen, J. Z., Caccuri, A. M., Antonini, G., Turella, P., Stella, L., Lo Bello, M., Federici, G., and Ricci, G. (2003) *J. Biol. Chem.* **278**, 42283-42293
24. Mannervik, B., Board, P. G., Hayes, J. D., Listowsky, I., and Pearson, W. R. (2005) *Methods Enzymol.* 401, 1- 8
25. Turella, P., Filomeni, G., Dupuis, M. L., Ciriolo, M., Molinari, A., De Maria, F., Tombesi, M., Cianfriglia, M., Federici, G., Ricci, G., and Caccuri, A. M. (2006) *J. Biol. Chem.* **281**, 23725-23732
26. Alberts, B., Johnson, A., Lewis, J., Raff, M., Roberts, K., and Watson, J. D. (2002) *Molecular Biology of the Cell*, pp. 661, Garland, New York
27. Caruso, F. (2004) *Colloids and Colloid Assemblies* (Caruso, F., ed) pp. 246-283, Wiley-VCH, Mannheim
28. Ai, H., Jones, S. A., and Lvov, Y. M. (2003) *Cell Biochem. Biophys.* **39**, 23-43

29. Hurst, R., Bao, Y., Jemth, P., Mannervik, B., and Williamson, G. (1998) *Biochem. J.* **332**, 97-100
30. Boese, M., Keese, M. A., Becker, K., Büsse, R., and Mülsch, A. (1997) *J. Biol. Chem.* **272**, 21767-21773
31. Becker, K., Savvides, S. N., Keese, M., Schimer, R. H., and Karplus, P. A. (1998) *Nat. Struct. Biol.* **5**, 267-271
32. Virtanen, I. (1978) *Cell Biol. Int. Rep.* **2**, 33-39

**4. STUDY OF GST OF MALARIAL
PARASITE (*Plasmodium falciparum*)**

3.6 Introduction

About two million deaths in the world are caused by *Plasmodium falciparum*, the parasite causative of tropical malaria (1, 2). In the scientific community, an increasing interest is now developing for the peculiar glutathione transferase (*Pf*GST) expressed by this parasite. *Pf*GST is one of the most abundant proteins expressed by this parasite (>1%, \cong 0.1 mM) (3) and differently from what occurs in many organisms, it is the sole GST isoenzyme expressed by this parasite. This specific isoenzyme cannot be assigned to any known GST class (3, 4) and the interest for this enzyme is due to its particular protective role in the parasite. In fact, beside the usual activity that promote the conjugation of GSH to electrophilic toxic compounds, this protein binds efficiently hemin and thus it could protect the parasite (that resides in the erythrocytes) from the parasitotoxic effect of this heme byproduct (5).

Specific compounds that selectively inhibit its catalytic activity or hemin binding could be promising candidates as anti malarial drugs. In this context, the discovery of structural or mechanistic properties of this enzyme that are not found in other GSTs may be of great relevance for designing selective inhibitors that are toxic to the parasite but harmless for the host cells. Two properties never observed in other members of the GST superfamily must be considered. The first one is that this enzyme, in the absence of GSH, inactivates in a short time and loses its ability to bind hemin (5). Recent studies indicated that the inactivation process is related to a dimer/tetramer transition (4). The second one is the strong positive homotropic phenomenon that modulates the affinity of the two subunits for hemin (5). The X-ray crystal structure of *Pf*GST, solved by two different groups, provides further details to understand this effect. From a structural point of view the most intriguing differences of *Pf*GST when compared to other GSTs are given by a more solvent-exposed H-site and by an atypic extra loop connecting helix-4 and helix-5 (residues 113-118) that could be involved in the dimer/dimer interaction. Actually, in the absence of ligands two dimers (AA1 and BB1) form a tetramer and these homodimers are interlocked with each other by the loop 113–118 of monomer B

(B1), which occupies the H-site of monomer A (A1) (6). Upon binding of S-hexylglutathione, the H-site loop 113-118 rearranges, residues Asn-114, Leu-115, and Phe-116 form an additional coil in helix-4 and the side chains of Asn-111, Phe-116, and Tyr-211 flip into the H-site. The changed course of the residues 113–120 in the liganded enzyme prevents the interlocking of the dimers; as a consequence, the molecules are packed as dimers (7).

In this study we have used site directed mutagenesis, fluorescence anisotropy and X-ray crystallography it will be checked the influence of selected mutations of this atypic loop in the tetramerization process, and the possible involvement of this protein segment in the positive cooperative phenomenon observed for hemin binding. In addition we show that the tetramerization process is inhibited not only by GSH but also by GSSG, which suggests that hemin binding and the catalytic competence of *Pf*GST are independent of the redox status of the cell. Finally it will be demonstrated that the presence of GSH (or GSSG) in the active site is not essential for hemin binding but this interaction only requires an active dimeric conformation.

4.2 Experimental Procedures

Materials - S-benzylglutathione, S-hexylglutathione, S-methylglutathione and hemin were obtained from Sigma-Aldrich.

Enzymes - *Pf*GST wild type and mutants, hinge-blocked with a substitution of residues 113 and 119 with two prolines (mutant A), point mutation Gln-118A (mutant C) and mini loop obtained by replacement of the entire protein segment 113-118 by a single alanine residue (mutant D), were expressed in *Escherichia coli* and purified as described previously (8). The purified forms of *Pf*GSTs were stored at -80 or 0°C in the presence of 10 mM GSH. Under these conditions, the enzymes were stable for weeks. Protein concentrations were calculated assuming an $\epsilon_{1 \text{ mg/ml}}$ of 1.1 at 280 nm for *Pf*GSTs on the basis of the amino acid sequence (9). A molecular mass of 25 kDa/GST subunit was used in the calculation (10).

Enzymatic activity - Standard *Pf*GSTs activity (wild type and mutants) was measured at 25°C in a 0.1 M potassium phosphate buffer, pH 6.5, containing 1 mM GSH and 1 mM CDNB. The activity was assayed spectrophotometrically by following the enzymatic product at 340 nm ($\epsilon = 9,600 \text{ M}^{-1} \text{ cm}^{-1}$).

Sephadex G-25 chromatography - (Size exclusion chromatography) - Gel filtration experiments were carried out on a Sephadex G-25 column (Pharmacia LKB, Uppsala, Sweden) to remove the storage GSH (10 mM). The column was equilibrated and run with 10 mM potassium phosphate buffer, pH 7.2, with a flow rate of 1 ml/min at 25°C. To see if GSSG could prevent enzyme tetramerization, the column was equilibrated and run with the above-mentioned buffer containing 1 mM GSSG.

Anisotropy experiments - Fluorescence anisotropy experiments were performed with a Spex Fluoromax 2 fluorimeter, using 280 nm excitation, 335 nm emission and 295 nm cut-off filter in the emission channel. Background signal was subtracted before anisotropy calculations, and the polarization response of the instrument was determined by measuring the G correction factor (1.78). Averages and standard deviations of anisotropy values were calculated from nine replicate experiments. 0.124 mg/ml protein concentration was employed in all experiments, and the effect of substrate binding was monitored by adding a 1 mM GSH concentration.

Isothermic binding of PfGSTs and Hemin - Isothermic binding data were following the quenching in the intrinsic fluorescence of PfGST ($\lambda_{ex}= 295$ nm; $\lambda_{em}= 333$ nm) caused by hemin binding. Data were fitted to the equation 1:

$$\vartheta = \frac{K + [\text{hemin}] + [\text{GST}] - \sqrt{(K + [\text{hemin}] + [\text{GST}])^2 - 4[\text{hemin}][\text{GST}]}}{2} \quad (1)$$

Inhibition of PfGSTs by hemin - Inhibition of PfGSTs by hemin was studied by adding variable amounts of hemin (from 0.2 to 10 μM) with a fixed enzyme concentration (1 μM), in 1 ml 0.1 M potassium phosphate buffer, pH 6.5 at 25°C. After about 10 seconds, 1 mM GSH and 1 mM CDNB were added for activity measurements followed at 340 nm. The data obtained by varying hemin concentrations were analyzed to the Hill equation 2:

$$v_i/v_{max} = [S]^n / (K^n + [S]^n) \quad (2)$$

where v_i is the initial velocity observed at a given concentration of hemin, v_{max} is the velocity observed in absence of inhibitor, $[S]$ is the hemin concentration, and n is the Hill coefficient at the hemin concentration corresponding to the half-enzyme saturation.

Inhibition data were also analyzed with a two-site Adair model (equation 3) for ligand binding to a homodimeric macromolecule to estimate K_1 (low affinity) and K_2 (high affinity) constants for hemin binding:

$$v_i/v_{max} = ([S] / K_1 + [S]^2 / \alpha K_1^2) / (1 + 2[S] / K_1 + [S]^2 / \alpha K_1^2) \quad (3)$$

where K_1 is the dissociation equilibrium constant for hemin binding to the free enzyme, αK_1 ($= K_2$) represents the dissociation equilibrium constant for hemin to the monoligated enzyme, and α is the non dimensional interaction parameter coupling the two functionally linked hemin binding sites.

4.3 Results

4.3.1 Kinetic properties of the loop113-118 mutants

Selected mutations of *PfGST* have been designed to evaluate possible involvement of loop 113-118 in the tetramerization process and in the cooperative phenomenon. In particular, in mutant D the entire protein segment 113-118 was replaced by a single alanine residue, the mutant C displays the single point mutation Gln-118A and in mutant A residues 113 and 119 have been substituted by two prolines to lower the flexibility of this protein segment. Expression of these mutant enzymes in *E. coli* and their purification are described in the “Experimental procedures” section. The three enzymes were then analyzed under steady state kinetic conditions and kinetic parameters compared to those of the native enzyme. As shown in Table 4.1 two mutants display a slight but significant loss of affinity for CDNB. This is not surprising as the loop 113-118 forms a part of the H-site. As expected, no relevant changes of affinity for GSH have been observed as a consequence of the single mutation and also of the truncation of the entire loop. Surprisingly, the hinge-blocked enzyme (mutant A) displays about four times lower affinity for GSH and about three times increased k_{cat} . This decreased affinity for GSH is unexpected as the loop does not interact directly with the G-site.

Table 4.1. Kinetic parameters of wild-type and various mutants of *PfGST* determined using CDNB conjugation assay

| <i>PfGST</i> ^a | K_m^{GSH} (mM) ^b | k_{cat}^{GSH} (sec ⁻¹) ^b | k_{cat}^{GSH}/K_m^{GSH} (M ⁻¹ sec ⁻¹) ^b | K_m^{CDNB} (mM) ^b | k_{cat}^{CDNB} (sec ⁻¹) ^b | $k_{cat}^{CDNB}/K_m^{CDNB}$ (M ⁻¹ sec ⁻¹) ^b |
|---------------------------|----------------------------------|--|--|-----------------------------------|---|--|
| Wild-Type | 0.15 ± 0.02 (100%) | 0.151 ± 0.007 | 1006 ± 50 | 2.2 ± 0.3 (100%) | 0.38 ± 0.02 | 173 ± 30 |
| Mutant A | 0.61 ± 0.05 (406%) | 0.413 ± 0.009 | 677 ± 60 | 5.1 ± 0.3 (232%) | 1.14 ± 0.03 | 223 ± 10 |
| Mutant C | 0.20 ± 0.02 (137%) | 0.122 ± 0.005 | 610 ± 60 | 3.3 ± 0.4 (150%) | 0.46 ± 0.02 | 139 ± 20 |
| Mutant D | 0.17 ± 0.02 (114%) | 0.160 ± 0.009 | 941 ± 100 | 2.4 ± 0.5 (109%) | 0.41 ± 0.05 | 171 ± 40 |

^a Given are mean values of three independent determinations and standard deviation.

^b The K_m for GSH and CDNB as well as the k_{cat} and the catalytic efficiency were determined using the CDNB conjugation assay.

4.3.2 Loop 113-118 modulates the kinetics of the inactivation process

Even slight perturbations of the loop 113-118 dramatically influence the kinetics of the inactivation process. In particular all these mutants display only a very small loss of activity as soon as GSH is removed by a Sephadex G-25 column, while the native enzyme undergoes about 50% inactivation (Fig. 4.1). Furthermore the second slower phase of inactivation observed in the native enzyme and that causes a total loss of activity after 24 h, is almost absent in these mutants. Thus, it appears that the inactivation process occurs at measurable rate only if the loop 113-118 is in a native conformation/sequence.

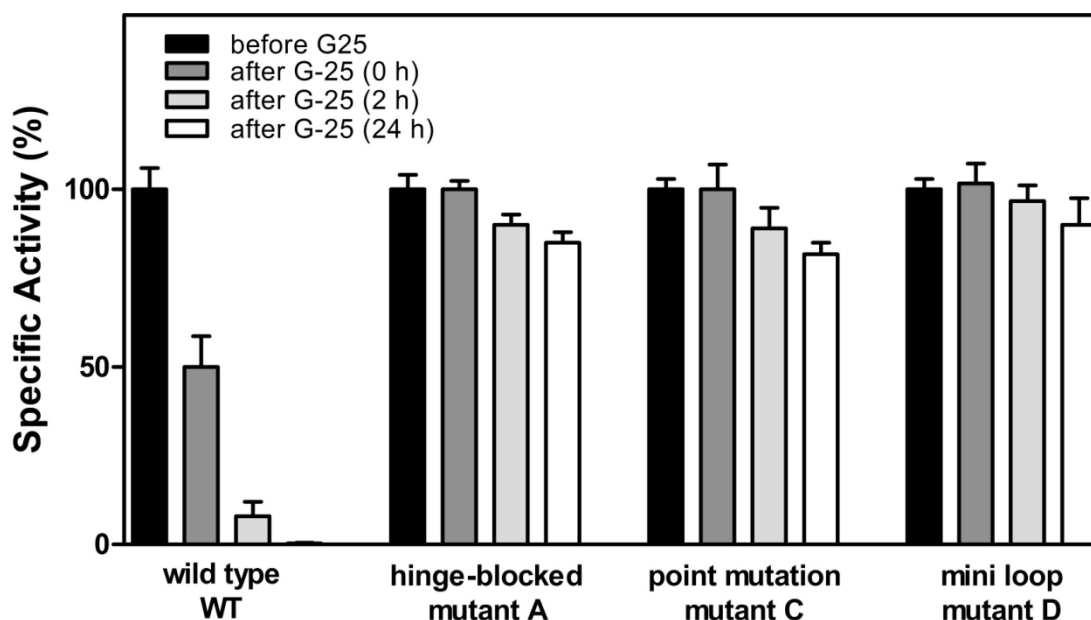


FIGURE 4.1 Inactivation of *PfGST* in the absence of GSH. Active dimeric *PfGST*s (with 10 mM GSH) were passed through a Sephadex G-25 column. After GSH depletion, the enzymatic activity was assayed as described under “Experimental procedures” section.

4.3.3 Tetramerization and inactivation are synchronous events

The tetramer *PfGST* is not active enzymatically (3). It is not clear if the tetramerization of *PfGST* observed in the absence of GSH is synchronous to the inactivation process or if these events occur with different kinetics. This detail could be important to define if the tetramerization is the cause or the effect of the loss of activity. Thus, the kinetics of tetramer/dimer transition triggered by GSH binding

(3) was studied by means of steady-state fluorescence anisotropy experiments and compared with the reactivation kinetics. Any attempt to follow the reverse reaction, *i.e.* the dimer/tetramer transition after removal of GSH was unsuccessful due to the very fast inactivation of this enzyme in the absence of GSH (5). Steady-state fluorescence anisotropy represents a useful approach to follow a dimer/tetramer transition since it provides a measure of the rotational motions of macromolecules. In the simplest case, when the protein diffusional motion can be modeled as the rotation of a rigid sphere, its value is related to the rotational diffusion time by the following equation: $r = r_0 / (1 + \tau/j)$ where τ is the fluorescence lifetime of the fluorophore contained in the macromolecule, and j is the rotational correlation time, which is proportional to the hydrodynamic volume of the protein and therefore depends on its aggregation state (11). Dissociation of a multimer results in a decrease in the fluorescence anisotropy value, due to the increase in rotational diffusion.

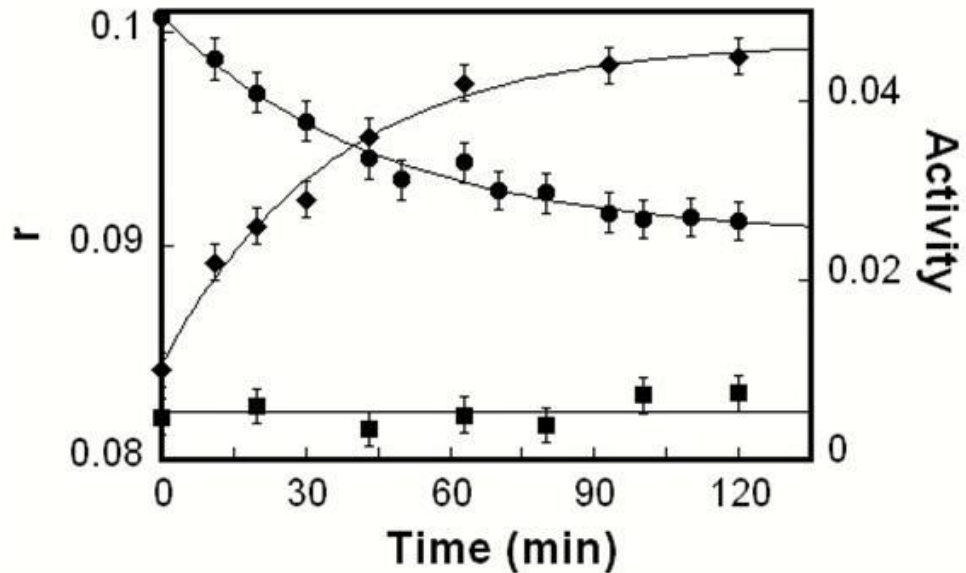


FIGURE 4.2. Steady state anisotropy fluorescence analysis. Inactive tetrameric *PfGST* wild type (5 μ M) obtained by GSH removal and 12 h incubation, was incubated with 1 mM GSH in 0.1 M potassium phosphate buffer, pH 6.5, at 25°C. At fixed times, fluorescence anisotropy (●) and enzymatic activity (◆), were monitored. Mutant (A) did not inactivate without GSH and did not show any significant change of fluorescence anisotropy (■) and activity (data not shown) after 1 mM GSH incubation. Mutants C and D show the same behavior as mutant A. Standard deviations of anisotropy values were calculated from nine replicate experiments.

In the case of the native *PfGST* the enzyme used is represented by the inactivated enzyme (tetrameric state) obtained after G-25 Sephadex chromatography and subsequent incubation at 25°C for 12 h in the absence of GSH. Incubation of this inactive enzyme with 1 mM GSH resulted in a decrease of the anisotropy values, accompanied by a parallel recovery of enzymatic activity (Fig. 4.2). The kinetics of the two processes could be fitted with the same first order kinetics, with a lifetime of 40 minutes, indicating a strict correlation between the two phenomena but no temporal priority. On the other hand, no appreciable change of the anisotropy given by the mutants, nor of their activity could be detected under the same experimental conditions, indicating that no change in the quaternary structure takes place as a consequence of substrate binding. The observed anisotropy value for the mutant is slightly lower than the plateau value of the wild type protein, but this could simply be due to a slight variation induced by the mutation in the average fluorescence lifetime of the protein (see equation 1), or in a different segmental mobility of some protein domains.

4.3.4 GSSG (and GSH-derivatives) inhibit the tetramerization process

A surprising property of *PfGST* is represented by its high affinity for the oxidized form of GSH. From kinetic inhibition data an apparent K_D value of 0.07 mM has been found for GSSG, a value even smaller than that for GSH (0.15 mM). GSSG behaves like a pure competitive inhibitor indicating that the protein counterpart must be identified as the G-site (Fig. 4.3 inset). Of particular interest is the influence of GSSG on the inactivation/tetramerization process. As shown in Fig. 4.3 the presence of GSSG (from 0.1 mM to 1 mM) prevents the inactivation process, thus stabilizing the dimeric structure. This means that *in vivo* the enzyme is able to retain its active conformation even when part of GSH is oxidized to GSSG, *i.e.* under oxidative insults. On the other hand, the inactive tetrameric enzyme does not restore its active conformation when incubated with 10 mM GSSG (Fig. 4.3), indicating that GSSG has a limited access to the G-sites of the tetrameric structure. As confirmation, no trace of quenching of the intrinsic

fluorescence has been found after addition of GSSG to the inactive form (not shown).

Other GSH derivatives like S-benzylglutathione and S-hexylglutathione also inhibit the tetramerization process with the only difference that S-benzylglutathione is very much more active in this prevention. As will be clear below, these results are in good agreement with those coming from X-ray crystal structures of wild type in complex with these inhibitors.

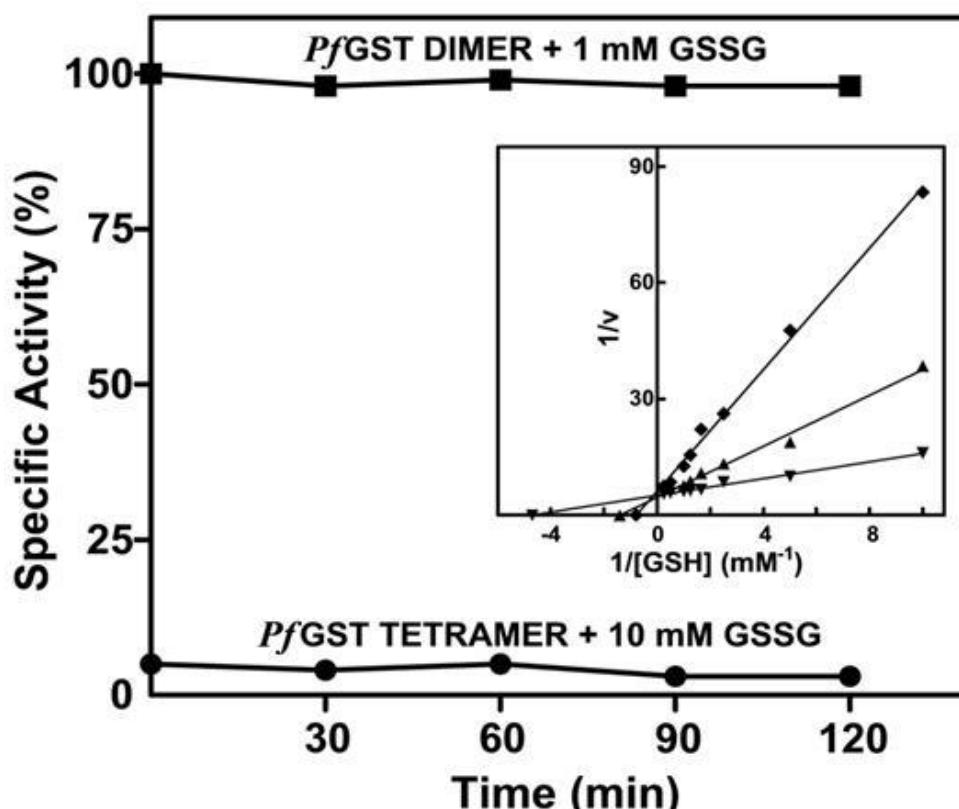


FIGURE 4.3. GSSG prevents both tetramerization and reactivation of *Pf*GSTs. (■) Active native *Pf*GST (2 mg) was passed through a Sephadex G-25 column saturated with 1 mM GSSG in 10 mM potassium phosphate buffer pH 7.2 at 25°C. Specific activity of enzyme was measured at different times at 25°C. (●) Inactivated *Pf*GST tetramer (2 mg) was incubated at 25°C with 10 mM GSSG. Inset: Lineweaver-Burk plot of $1/v$ versus $1/[GSH]$ obtained by adding variable amounts of GSH (from 0.1 to 4 mM) to the native *Pf*GST in the presence a fixed GSSG concentrations: (■) 0.53 mM, (σ) 0.23 mM and (τ) 0.03 mM) in 1 ml of 0.1 M potassium phosphate buffer, pH 6.5 (25°C).

4.3.5 The integrity of the loop 113-118 is essential for the positive cooperativity in hemin binding

*Pf*GST displays a positive homotropic behavior for hemin binding so that the affinity of the vacant subunit increases about twenty times when one hemin molecule binds to the first subunit of the dimer (5). This modulation has been interpreted as finalized to optimize the interception of the toxic hemin by the parasite that living in erythrocytes is likely exposed to this heme byproduct. Other GST isoenzymes (Alpha, Mu and Pi isoenzymes) equally able to bind this compound, display a non-cooperative interaction (Table 4.2). The availability of specific mutants for *Pf*GST makes it possible to determine the influence of the loop 113-118 in the cooperative phenomenon. As shown in Table 4.2, the loop 113-118 is crucially involved in the intersubunit structural communication; in fact all mutants have lost or strongly lowered the cooperative behavior, showing an Hill coefficient near the unit (Table 4.2).

Table 4.2. Binding of hemin to *Pf*GST calculated from inhibition data^a.

| <i>Pf</i> GST | n_H | $K_{D\ app}$ (μ M) |
|----------------------------|---------------|--|
| Wild Type (G) ^b | 1.9 ± 0.1 | K_1 (low affinity) = 2.8 K_2 (high affinity) = 0.16 |
| Hinge blocked (A) | 1.2 ± 0.2 | 0.46 ± 0.03 |
| Point mutation (C) | 1.1 ± 0.1 | 0.15 ± 0.01 |
| Mini loop (D) | 1.0 ± 0.1 | 0.22 ± 0.02 |
| GSTP1-1 | 1.1 ± 0.1 | 0.10 ± 0.02 |
| GSTA1-1 | 1.0 ± 0.2 | 0.060 ± 0.003 |
| GSTM2-2 | 1.0 ± 0.1 | 0.11 ± 0.02 |

^a Inhibition data fitted to the Hill equation $v_i / v_{max} = [S]^n / (K^n + [S]^n)$

^b Data from Ref (5), were K_1 and K_2 were obtained by fitting experimental data to the Adair equation

Analysis of the dissociation constants calculated from inhibition experiments shows that all these mutants (in the presence of GSH) display an affinity very similar to that of the high affinity binding site of the native enzyme observed when hemin has hemisaturated the dimer (see Table 4.2). These findings were also confirmed by isothermic binding data coming from fluorescence experiments

(Table 4.3), although in the absence of CDNB, all dissociation constants are translated toward lower values.

4.3.6 GSH is not essential for hemin binding

*Pf*GST is able to bind hemin only when the enzyme is in the active dimeric structure *i.e.* in complex with GSH (5). Due to the fast tetramerization of the enzyme in the absence of GSH, it remains uncertain if the hemin binding is prevented by steric hindrance given by the tetrameric structure or by the absence of GSH in the G-site. The particular inertness of the mutated enzymes that tetramerize very slowly in the absence of GSH makes it possible to clarify this question. Binding of hemin can be visualized on the basis of the quenching of intrinsic fluorescence. The results reported in Table 4.3 and Fig. 4.4 indicate that all mutants are able to bind hemin even in the absence of GSH.

Table 4.3. Isothermic binding of hemin to *Pf*GSTs (fluorescence experiments).

| <i>Pf</i> GST ^a | | n_H^a | K_D (μ M) ^a |
|----------------------------|----------------|---------------|--|
| Wild-Type (G) ^b | (1 mM GSH) | 1.7 \pm 0.1 | K_1 (low affinity) = 1.3 K_2 (high affinity) < 0.08 |
| Wild-Type (G) | (1 mM GSSG) | 1.1 \pm 0.2 | 1.9 \pm 0.1 |
| Wild-Type (G) | (0.01 mM GSSG) | 1.0 \pm 0.2 | 1.5 \pm 0.2 |
| Hinge blocked (A) | (1 mM GSH) | 0.9 \pm 0.1 | < 0.1 |
| Hinge blocked (A) | – | 0.9 \pm 0.1 | 1.3 \pm 0.1 |
| Point mutation (C) | (1 mM GSH) | 1.0 \pm 0.1 | < 0.1 |
| Point mutation (C) | – | 1.1 \pm 0.2 | 0.9 \pm 0.1 |
| Mini loop (D) | (1 mM GSH) | 1.1 \pm 0.1 | < 0.1 |
| Mini loop (D) | – | 1.0 \pm 0.1 | 1.9 \pm 0.1 |

^a Inhibition data fitted to the Hill equation $v_i / v_{max} = [S]^n / (K^n + [S]^n)$

^b Data from Ref (5), where K_1 and K_2 were obtained by fitting experimental data to the Adair equation

However the affinity is lower than that found in the GSH-enzyme complex. Thus, all these mutated enzymes display two different conformations characterized by two different affinities for hemin (one high affinity conformation, R-state and one low affinity conformation, T-state) determined by the presence or absence of GSH. Finally, we also observed that the native enzyme is able to bind hemin even in the presence of GSSG. In this case the binding is non-cooperative and the

dissociation constant indicates a low affinity conformation. This behavior parallel that observed in the presence of S-methylglutathione (5) and indicates that the free thiol group in the active site is important for the cooperative mechanism. The ability of *Pf*GST to bind hemin in the presence of GSSG is also of physiological relevance as it demonstrates that this enzyme may protect the cell from hemin even under severe oxidative stress conditions.

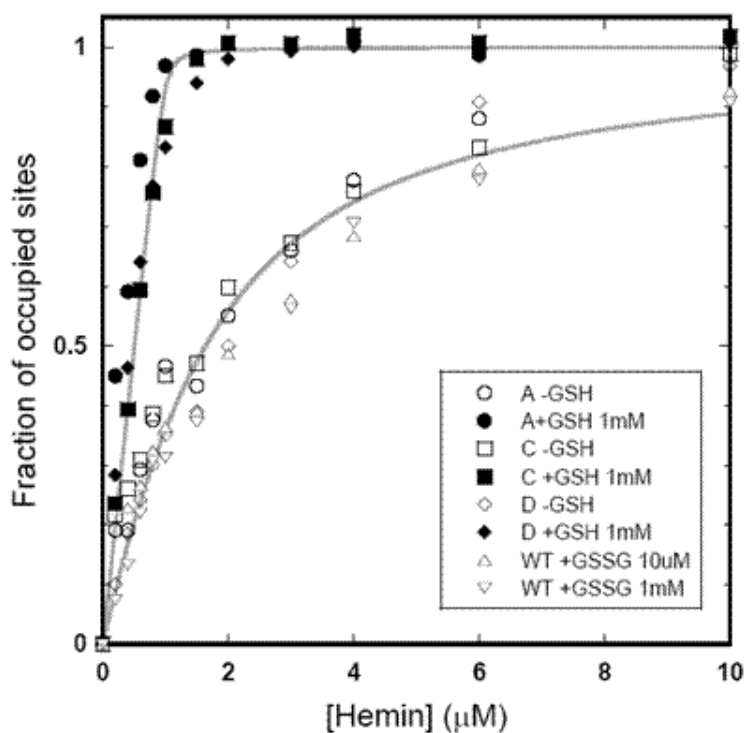


FIGURE 4.4. Isothermic binding of hemin to WT and mutants *Pf*GSTs (fluorescence experiments). Variable amounts of hemin (from 0.2 to 10 μM) were added to *Pf*GSTs (1 μM) in the presence or absence of 1 mM GSH, 1 mM GSSG and 0.1 mM GSSG in 0.1 M potassium phosphate buffer, pH 6.5, at 25°C. Quenching of the intrinsic fluorescence was measured as described in “Experimental Procedures” section and data were fitted to the Equation 1.

4.3.7 X-ray crystal analysis

X-ray crystal analyses add further details. All three mutants crystallized in the absence of GSH display tetrameric structures very similar to that observed when the native enzyme crystallizes in the apo-form. This is not surprising as all present data indicate that tetramerization is not thermodynamically prohibited for all these mutants but only slowed (Fig 4.1). Actually, crystallization requires high enzyme

concentrations and several days growth. Nevertheless, if we compare the structure of the dimeric *PfGST* in complex with GSH and its tetrameric apo form, one interesting difference is the switch of the loop 113-118 hinged by Tyr-113 and Asp-119 that rotates about 30 degrees and that in the tetrameric structure occupies the H-site of the adjacent dimer (Fig. 4.5).

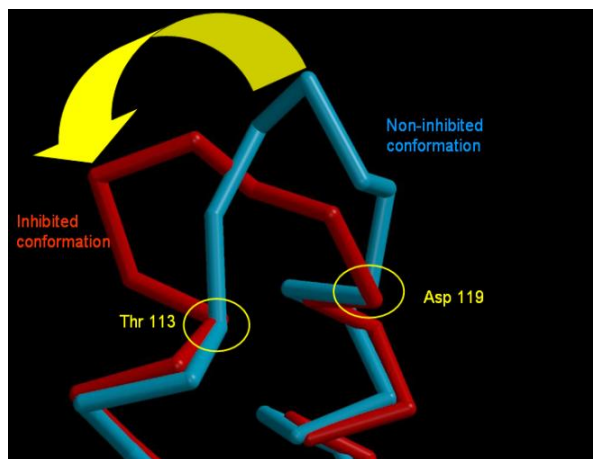
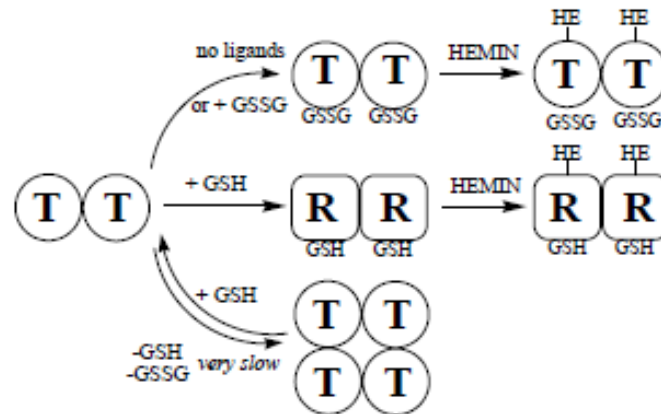


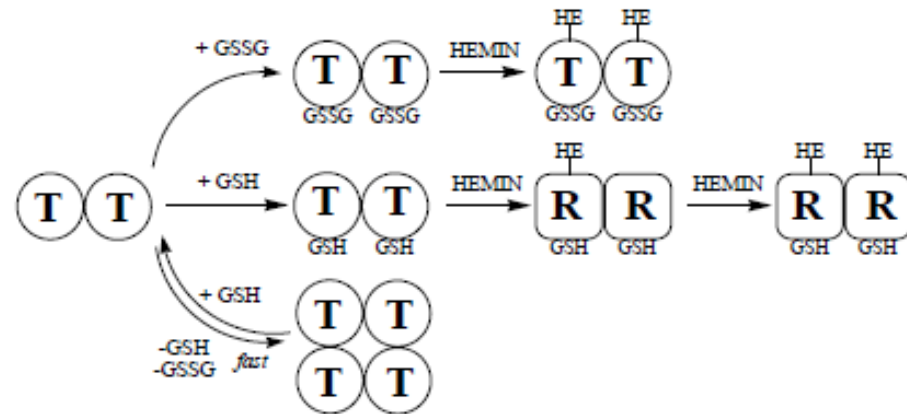
FIGURE 4.5. Loop movement upon substrate binding. In the non-inhibited state (*blue*) loop 113-119 reveals a different conformation than in the inhibited state (*red*).


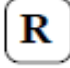
It appears that the structural transition of this loop from the A conformation to the B conformation is propedeutical to the tetramerization event, but it may also be linked to the high-low affinity transition for hemin binding (T→R transition). We remember that Asn-112 is likely involved in the hemin stabilization through coordination to the iron atom (5), so it is not surprising that any structural change of the loop 113-118 may cause so relevant effects for the hemin binding. All these structural observations, together with all kinetic data will be combined in the Scheme 4.1 that represents a possible explanation.

*Pf*GST MUTANTS:



*Pf*GST WILD TYPE:



-  = low affinity conformation for Hemin
-  = high affinity conformation for Hemin

SCHEME 4.1

4.4 Discussion

A few structural and functional properties of *Pf*GST make this enzyme unique in the wide scenario of GSTs in living organisms. One of these is represented by the peculiar tetramerization that causes complete inactivation of the enzyme and that occurs in a few minutes in the absence of GSH. Our data showed that this event becomes very slow when selected mutations have been introduced in the loop 113-118. Thus it is now clear that the integrity of loop 113-118 is essential for this process. However the possibility that tetramerization may occur *in vivo* is remote. Data reported here demonstrate that besides GSH, even GSSG is able to slower drastically the inactivation. Thus even under conditions of severe oxidative stress for the parasite, the tetramerization does not occur unless unknown endogenous or exogenous compounds promote this event. On the other hand, the peculiar loop 113-118 seems to have crucial relevance in the hemin binding of *Pf*GST, and in particular in the cooperative phenomenon that characterizes this interaction. In fact the positive homotropic behavior triggered by hemin itself disappears completely if this loop is truncated, stiffened or slightly modified by a single point mutation. Furthermore, the presence of GSH in the G-site is not essential for hemin binding, but in its absence all mutated enzymes show a lower affinity for hemin and a non-cooperative binding.

Interestingly, a non-cooperative shift toward a high affinity conformation for hemin is triggered by GSH in all mutants but not in the native enzyme where both subunits remain in the low affinity conformation until a hemin molecule is bound to one subunit. Considering that other GST isoenzymes like Alpha, Pi and Mu bind hemin in a non-cooperative behavior, and with an affinity similar to that of the high affinity binding site of *Pf*GST (Table 4.2), it seems that a high propensity to bind hemin is a common property of many GSTs and that a more efficient hemin binding by *Pf*GST could easily have been obtained during evolution, even by a single point mutation. Thus it appears that cooperativity in the parasite is finalized to decrease the affinity for hemin at low hemin concentrations and not to increase its intrinsic affinity. This strategy seems plausible considering that the parasite living in the

erythrocyte is likely exposed to free hemin and that the *PfGST* is completely inactivated when it has bound hemin. In other terms, due to the particular environment of *Plasmodium falciparum*, this enzyme could be evolved to preserve the classical detoxicating activity as long as the free hemin concentration is harmless to the cell. In any case, the conservation of the unique loop 113-118 in *PfGST* demonstrates that this structural element is essential for the correct functioning of the enzyme in these parasites. The absence of this loop in mammalian GSTs means that inhibitors interacting at this site will be highly selective for the Plasmodium transferase.

This mechanism parallels the cooperative behavior of hemoglobin that evolved from an ancestral globin at high affinity (similar to myoglobin) to reach the tetrameric cooperative protein that, at low oxygen pressure, shifts toward a lower affinity conformation promoting the oxygen release at level of tissue.

4.5 References

1. Breman, J. G. (2001) *Am. J. Trop. Med. Hyg.* **64**, 1-11
2. Greenwood, B., and Mutabingwa, T. (2002) *Nature* **415**, 670-672
3. Tripathi, T., Rahlfs S., Becker, K., and Bhakuni, V. (2007) *BMC Struct. Biol.* **7**, 67
4. Becker, K., Tilley, L., Vennerstrom, J. L., Roberts, D., Rogerson, S., and Ginsburg, H. (2004) *Int. J. Parasitol.* **34**, 163-189
5. Liebau, E., De Maria, F., Burmeister, C., Perbandt, M., Turella, P., Antonini, G., Federici, G., Giansanti, F., Stella, L., Lo Bello, M., Caccuri, A. M., and Ricci G. (2005) *J. Biol. chem.* **280**, 26121-26128
6. Wolf, K. F., Becker, A., Rahlfs, S., Harwaldt, P., Schirmer, R. H., Kabsch, W., and Becker, K. (2003) *Proc. Natl. Acad. Sci.* **100**, 13821-13826
7. Hiller, N., Wolf, K. F., Deponte, M., Wende, W., Zimmermann, H, and Becker, K. (2006) *Protein Sci.* **15**, 281-289
8. Harwaldt, P., Rahlfs, S., and Becker, K. (2002) *Biol. Chem.* **383**, 821-830
9. Gill, S. C., and von Hippel, P. H. (1989) *Anal. Biochem.* **182**, 319-326
10. Liebau, E., Bergmann, B., Campbell, A. M., Teesdale-Spittle, P., Brophy, P. M., Luersen, K., and Walter, R. D. (2002) *Mol. Biochem. Parasitol.* **124**, 85-90
11. Lakowicz, J. R. (2006) *Principles of Fluorescence Spectroscopy*, pp. 353-382 Springer, New York

CONCLUDING REMARKS

The common denominator of the studies reported in the present thesis is represented by the discovery of new protective mechanisms of the GST superfamily, mainly due to new ligandin properties of these enzymes. These particular non-enzymatic roles are possible because of the high expression of GSTs in cells of many different tissues and organism (0.8 mM in hepatocytes). The present study enlarges the scenario of cell protection given by GSTs. In particular our results indicate that GSTs of rat hepatocytes are deeply involved in the cell protection against excess of NO. In fact GSTs (in particular of Alpha class GSTs) represent the prime target for DNDGIC, a paramagnetic compound that is spontaneously and quantitatively formed when NO enters the cell. This complex would inactivate glutathione reductase but becomes completely harmless when bound to GSTs. Thus for the first time GSTs appears as a potent protection buffer against NO insults. In this context the interesting discovery that a significant amount of the cytosolic Alpha GST is electrostatically bound near to nuclear membrane (as proved by confocal microscopy, immunostaining experiments, and molecular modeling) may be interpreted as an additional protection shell for the precious genetic material that resides inside the nucleus. Finally, the molecular details concerning the peculiar GST isoenzyme expressed by the *Plasmodium falciparum* indicate that this enzyme evolved to sequester efficiently the toxic hemin only when this compound exceeds a critical concentration. This property, never before found in other GSTs, is possibly finalized to preserve the enzymatic activity of this GST at non-toxic hemin concentration. It is based on a cooperative mechanism that is active only when a particular protein segment (loop 113-118) is unperturbed.